Effects of Physical and Electrical Parameters on Damage Caused by Electrical Arcing

William Linzey, Michael Traskos, and Armin Bruning
Lectromechanical Design Company
45,000 Underwood Lane
Sterling, Virginia 20166
Phone: (703) 481 – 1233
Fax: (703) 481 – 1238

Michael Walz, and Cesar Gomez
Aging Aircraft Electrical Systems
Federal Aviation Administration
William J. Hughes Technical Center AAR-480
Atlantic City International Airport, NJ, 08405
Phone: (609) 485 - 8493

1 ABSTRACT

The amount of damage that can be caused by electrical arcing events continues to be an important question for both new and legacy aircraft. Many factors can affect the damage done by arcing events. For example, events occurring a short distance from a power bus can have much higher currents and power than those a long distance from the bus. Other important parameters include voltage, target material and geometry, circuit protection, separation, wire gauge and specification, initiation method etc. Over 600 arcing tests have been performed with varying physical and electrical conditions that would likely be experienced on in-service aircraft. The resulting damage to the arcing target and wires in the test bundles have been measured as well as the power and energy dissipated in the arc. This data has been compared with arcing data previously generated by the FAA Tech Center. Analyses of both sets of data have identified how variations in physical and environmental parameters affect the resulting damage. This paper will summarize the results of these tests and trends that have been found. This data will serve as the basis for an arc damage modeling software tool that is currently under development.

2 EXECUTIVE SUMMARY

This report covers the first stage of the work done in the construction of an Arc Damage Modeling Tool. The goal of this first task of the four task project, was to generate electrical arcing data that that will be used in the remainder of the project to help define and model arcing events. To this end, 205 different test configurations were used, totaling to 719 individual tests. These tests included variations in wire specification, fault currents, targets, and other variables that were deemed to be of interest or would modify the level of arcing damage to targets such as structure and hydraulic lines.

Methods were developed to assess the damage to the arcing targets and the wires causing damage. A large number of tests resulted in the penetration of hydraulic lines. These tests not only included those with high energy arcs and large diameter wires, but also small gauge wires with lower energy arcs.

The type of wire insulation had an effect on the damage done by the arc with wire that did not contain any polyimide showing the least damage. However, all wire types created damage in at least some cases.

Using a 28 VDC source voltage, arcing can penetrate an aluminum tube. This occurred more frequently with larger wire gauges (>20 AWG) and fault currents (> 400 amps).

The use of the wire strand mesh and target wires placed above an arcing wire bundle proved effective in determining the effective damage radius of the arc plume. Tests indicate a damage distance of between ¼ and ¾ inches. Profiles of the arc plume were also captured with this method.

A vibration arc initiation method was developed and proved to be a useful test, particularly in extending the duration of arcing events (by creating repeated strikes on the target, not one sustained arcing event). One of the disadvantages of this test however, was the long time necessary to setup the test compared to the other arc initiation methods.

In many of the tests, the arc fault circuit breakers (AFCBs) used limited the damage done to the target. However, in a few of the test performed, the arcing was sufficient to penetrate the walls of hydraulic lines in spite of being protected with an AFCB.

3 INTRODUCTION

The purpose of the Task 1 of this four phase project, was to develop the empirical framework required to then develop a model of the damage done in arcing event aboard aircraft. The data collected will be used in an attempt to quantify, as fully as possible, the power/energy dissipated in the arc and the damage caused by the arc. The damage done by the arc included damage done to the target (what is arced), the source wire(s), other wires in the bundle and other wires or objects at a distance. The parameters included in the testing were varied to cover the widest range of arcing scenarios that could realistically occur on an aircraft

The majority of the testing was done at the Lectromec lab using a 20 kVA permanent magnet generator. However, this machine could not produce fault current much in excess of 500 Ampere. Because high currents can be found near the aircraft power buses, especially in larger gauge wire, a series of tests were perform at the FAA Tech Center AFL using a 140kVA generator with setup that had 1100 to 1200 fault currents.

3.1 BACKGROUND – IN-SERVICE INCIDENTS

To insure the development of the arc damage modeling tool is developed so that in corresponds to arcing events that occur in the field data was gathered about arc events that were found on in-service aircraft. This work was performed by Mr. George Slenski and the Cessna Aircraft Company independently. For each of these events noted, information about the power system, wire gauge, and some means of assessing the amount of damage to the target and wire were needed for a comparison to be made.

Other events were presented in the evaluation, but are not described herein as there was not sufficient information to determine the conditions of the incident. The following includes two examples of well recorded electrical wire incidents and the resultant damage caused in each case.

3.2 INCIDENT #1

A bundle containing 12 gauge 115 VAC power wires and protected with a three-phase 15 ampere thermal circuit breaker chafed to a high pressure titanium (typically alloy 3AI-2.5V) hydraulic line in a location rarely accessed by maintenance personnel (Figure 1).

Figure 1. Failure initiation site is shown in the white box. Note that the wire bundle is lying on the hydraulic line. Red anti-chafe tape was used to protect the wiring.

The wire bundle was laying on the hydraulic line and vibration of the wire bundle on the hydraulic line couple chafed through the wire insulation. Exposed conductors arced to the titanium hydraulic line. Arcing was sufficient to breach the titanium tube, releasing 4,000 PSI hydraulic fluid that was subsequently ignited by continued arcing. Most damage to the remaining wiring, and loss of multiple systems, was due to external heating by a flame fueled by the spraying hydraulic fluid. Two 115 VAC three-phase 12 gauge wires arced to the hydraulic line. The 15 ampere thermal circuit breakers protecting the wires tripped at some point during the failure. A close-up of the wires that arced to the hydraulic line is shown in Figure 2.

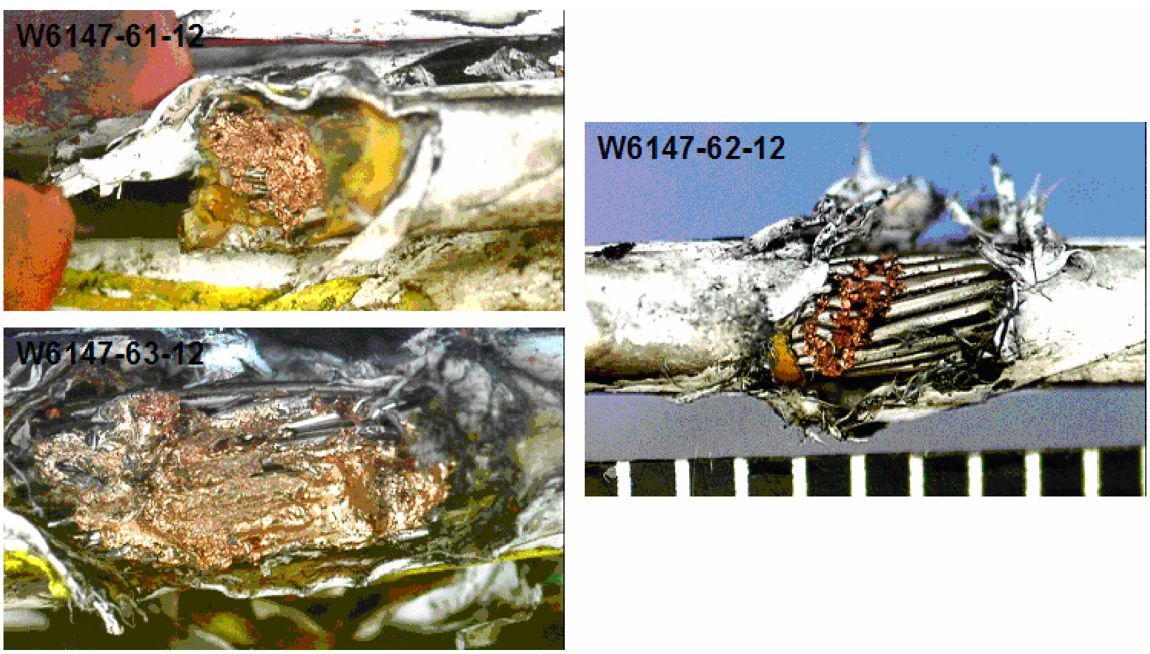

Figure 2. Close-ups of individual 115VAC fuel boost pump wires Phase A (top left), Phase B (middle right), and Phase C (bottom left). Phase A and C wires show evidence of arcing and melted conductors. The phase B wire only had damage from a flame source and mechanical abrasion.

The arc initiation site on the hydraulic line is shown in Figure 3, which shows the pinhole location in the hydraulic line and chafe areas on the composite couple. Note the broken composite fibers near the tube-couple interface. The hydraulic line pinhole location exhibited molten material with areas rich in copper from the arced wires (transfer of copper to the target was seen in many of the Task #1 tests).

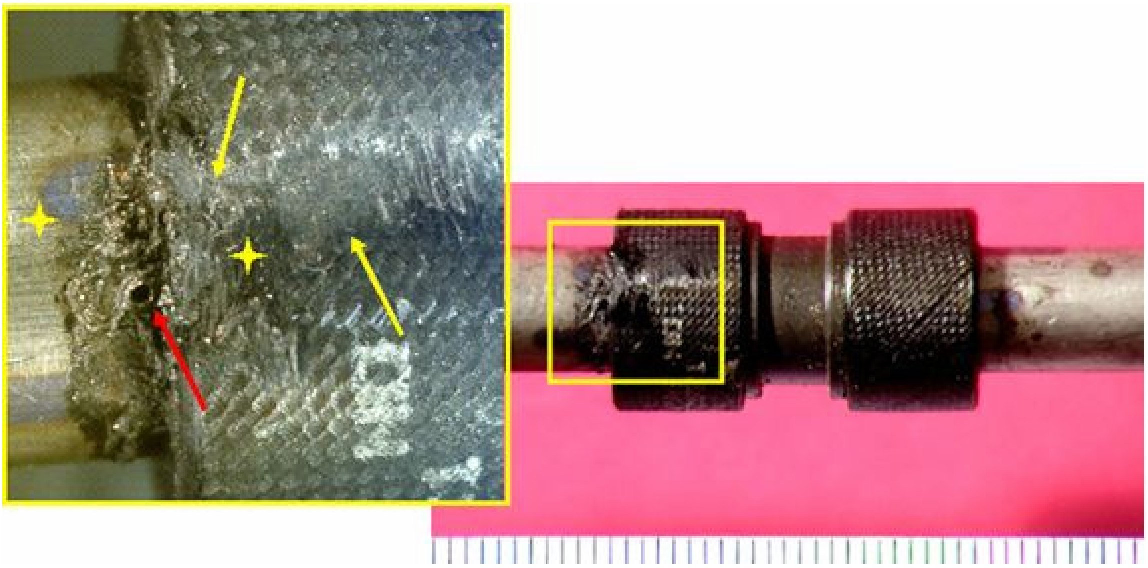

Figure 3. Arc initiation site on hydraulic line is shown in the yellow box. Red arrow in close-up photo highlights pinhole location; yellow arrows highlight chafing of coupling composite. Note the broken composite fibers near the tube-couple interface. A conductive path was measured between the yellow stars.

Note how the tube wall extruded outward resulting in a wall rupture (Figure 4). Calculations show that a 0.5 inch diameter titanium hydraulic line pressurized at 4000 PSI would rupture at approximately 454°C (850°F) which is well below the melting of titanium (1668°C or 3034°F). A surface temperature of 454°C (850°F) was well exceeded.

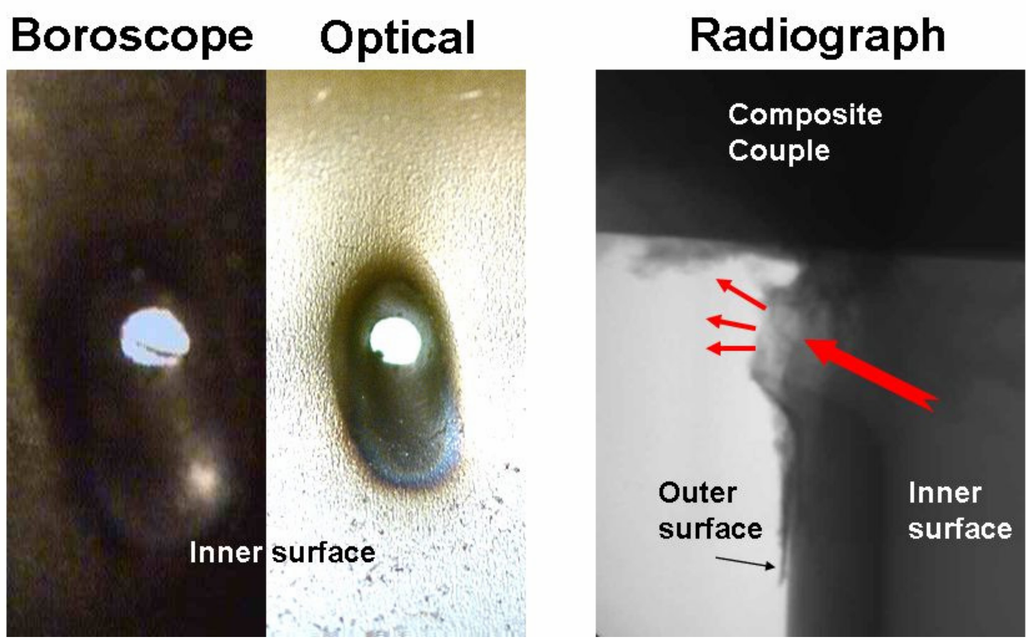

Figure 4. The cone shape of the failure site indicates a rupture failure of titanium wall while under pressure (4000 psi). Calculations show a 0.5 inch TI hydraulic tube at 4000 PSI would rupture at approximately 850°F (454°C).

3.3 INCIDENT #2

In another incident, mishap investigators located the damaged hydraulic line shown in Figure 5 (aluminum (6066) hydraulic line). Erosion from arcing penetrated the 3,000 PSI pressurized hydraulic line. High velocity fluid that sprayed from the breach was ignited and heat from the fire destroyed surrounding wiring and structure. The mishap hydraulic line was examined with a scanning electron microscope and Energy Dispersive Spectroscopy (EDS). In this case, SEM inspection with EDS confirmed the melting of the aluminum and presence of copper from copper wiring at the suspected arc damage site (Figure 6).

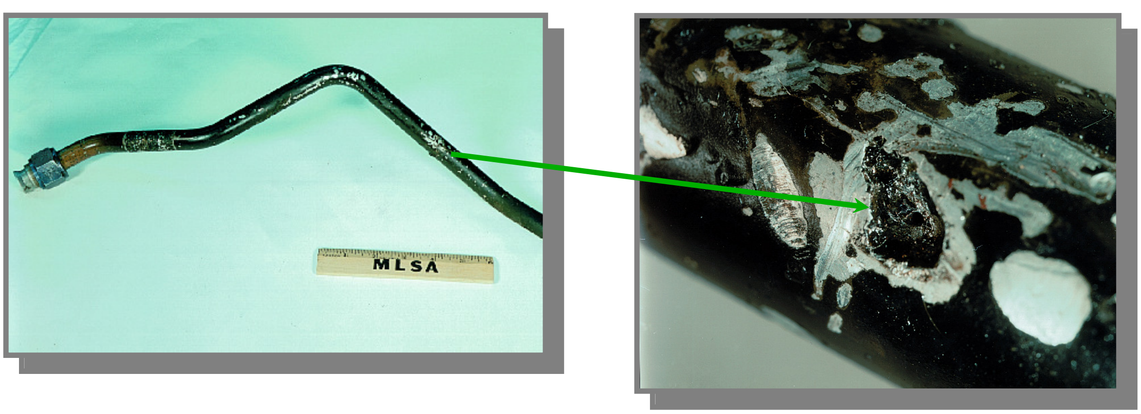

Figure 5. Arced aluminum hydraulic line removed from electrical fire area. Note arc site (lower right) that penetrated the aluminum wall.

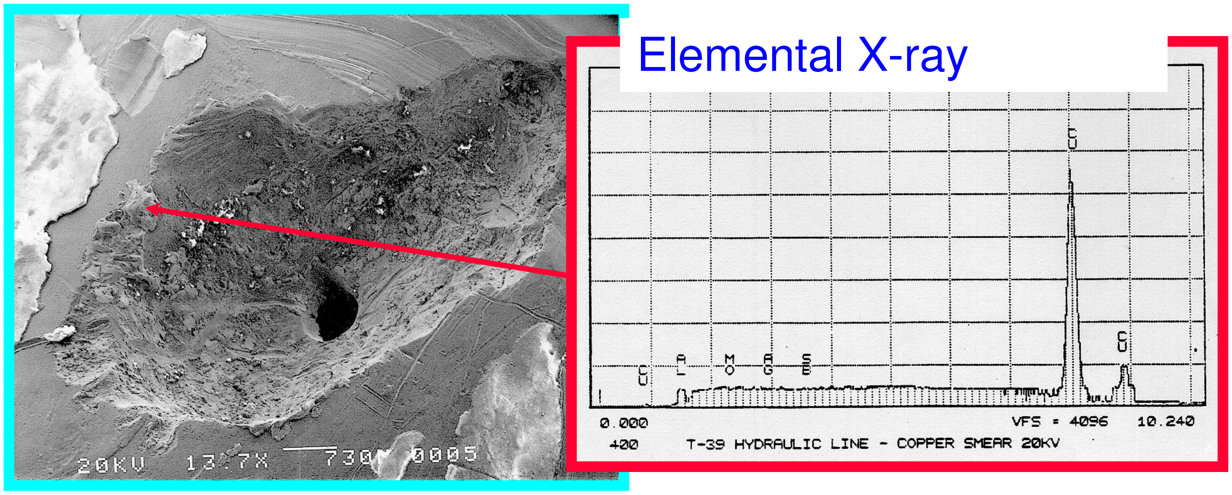

Figure 6. Close-up of the mishap hydraulic line arc site shows complete wall penetration. The size of the arc site is approximately 0.25 inches square. A round hole in the arc site was created by an onsite mishap investigator placing a safety wire through the breach in the hydraulic line. The upper left and right SEM micrographs show melting of the aluminum and the presence of copper (white areas in upper right). EDS (lower right confirms the presence of copper (Cu) in the arc site.

Inspection of wiring located in the electrical fire identified a wire with arcing evidence. The 16 gauge wire was one phase of a 115 VAC three-phase circuit. A close-up the arc site is shown in Figure 6. Note the small size of the copper wire arc site, 0.060 inches (Figure 7) compared to the arc site of the aluminum line which was 0.25 inches (Figure 6). Arcing to the copper wire was confined to several strands and contained aluminum when examined with an SEM using EDS.

Figure 7. Close-up of copper wire found in electrical fire with arcing damage. Note small arc site compared to the aluminum hydraulic line in figure 17. SEM micrographs show the arcing was confined to several strands. EDS analysis found aluminum in the arc area.

3.4 INCIDENT #3

In this incident a wire bundle chaffed against a hydraulic line and caused an electrical arc that breaches the hydraulic line and set the leaking hydraulic fluid on fire. The arcing wire was a 12 AWG feeder, powered with 115 VAC that was directly connected to the alternator with no circuit protection. The hydraulic line was made of 6061-T6 aluminum and had a wall thickness of 0.035 inches. The hole in the hydraulic line was 0.09" by 0.12".

4 TASK #1 – EMPIRICAL APPROACH

The purpose of Task #1 was to conduct a series of arcing tests that would be representative of arcing that could occur on an aircraft. The test parameters were varied to include a wide range of possible arcing scenarios. The tests were instrumented to collect the arcing voltage and current data. The damage done to the target, active wire, passive wire and targets at a distance were measured and quantified. The following section outlines the test methods and results

4.1 TEST MATRIX

The test matrix consisted of 205 different test groups with each test group usually containing 3 or more individual tests for a total of 719 tests. Table 1 lists the different parameters that were varied and the number of tests in which a particular value of the parameter was used.

Table 1. Breakdown of the parameters used in testing and the number of tests (Count) in which each parameter was used.

Source Voltage		Initiation Method		Fault Current (A)		Circuit Protection		Target	
Value	Count	Value	Count	Value	Count	Value	Count	Value	Count
115 AC	624	Swing	299	250	244	7.5 A Th	356	3/8" Al Tube	249
28VDC	42	Guil (BG)	151	500	227	7.5A AF	171	1/8" Al Rect	160
3Ph AC	42	Wet	123	100	132	20 A Th	89	PI-Wire	87
115AC/28VDC	11	Vib	94	1100	57	20A AF	26	FCC	55
		Guil (BF)	52	50	17	15A AF	23	1/2" Ti Tube	53
				400	12	5 A Th	18	Spar	36
				300	10	15 A Th	15	TGS	23
				200	8	5A AF	13	1/16" Al Rect	22
				600	8	3 A Th	3	Razor Blade	21
				25	4	1 A Th	2	XL-ETFE-Wire	7
						8A F	2	BMS1360-Wire	6
						3A F	1		
Active Wire Insulation		Active Wire Gauge		Passive Wires Insulation		Segregation Material		Dirt and Debri	
Value	Count	Value	Count	Value	Count	Value	Count	Value	Count
PI	601	20	527	PI	446	No	686	No	709
XL-ETFE	35	14	122	XL-ETFE	128	10mil Teflon	15	Yes	10
BMS1360	33	10	33	BMS1360	59	Round-It	9		
DK	18	24	28	DK	30	PPS/Silica	9		
CF	16	16	9	CF	28				
XL-PA	16			XL-PA	28				

4.1.1 TEST VARIABLES

The test parameters were selected to best represent those variables which were believed to have the greatest effect on arcing and also those that cover the greatest number of aircraft environments. A short explanation of the test parameters is given in the next sections.

A.1.1 INITIATION METHODS

The vibration, swing and guillotine test are variations on dry arc initiations. They all initiate the arc by metal–to-metal contact that is drawn apart. Therefore, while the type insulating may affect the arc, an arc can occur regardless of the wire insulation. These types of arcs are responsible for most of the arcing reported on aircraft due to chaffing etc.

The vibration test represents the scenario where a harness is in contact with a vibrating metallic piece of the aircraft that chafes through the wire insulation and an arc ensues. The swing test represents a scenario in which a harness sways or bumps into a metallic aircraft part. The guillotine test represents a pinch or cut-through scenario. The guillotine tests were done two ways: one in which the blade was grounded and arcing to one active wire. The second method followed the AS5692 guillotine test method more closely in which the floating blade bridged the gap between two pre-damaged wire in the test bundle.

The main purpose of the dry initiation tests was to measure the amount of damage to both the target and the arcing wire. Because the direction of the arc was away from the harness, it was thought that the damage to the other wires in the harness would be limited. However, after the first set of tests, it was found that the guillotine test with grounded blade did as much damage to other wires in the harness as the wet initiation method. The guillotine test with grounded blade method was then used as a measure of damage to other wires in the bundle in subsequent tests.

There are two important damage quantifications to be made with the Wet arc tests. The first is to the other wires in the harness. The second damage measurement was to wires and other objects at different distances, up to 1 inch, from the arcing harness.

A.1.2 FAULT CURRENT

The fault current is defined as the peak current that was measured if the test circuit was shorted at the specimen. The fault currents were chosen to represent the range of fault currents that could be found on an aircraft. The capacity of the generator and the resistance of the wire between the generator and the fault determine the fault current. When the fault current is 500 amps or below the resistance of the wire is the primary factor in limiting the current. When above 500 amps, the source impedance of the generator is the more significant factor. For example, to limit the fault current to 100 amps (peak) there would need to be about 176 feet of 20 AWG wire between the fault location and the power bus. Since there are few, if any, wire longer than this on an aircraft, this is the lowest fault current tested for 20 AWG wire. Adding lengths of wire in series with the arc controlled the fault currents for the individual test. The range of faults currents varied for the different wire gauges and source voltages.

A.1.3 CIRCUIT PROTECTION (TIME TO TRIP)

The circuit protection acted to limit the duration of the arcing event. There were two different kinds circuit protections used; the traditional thermal circuit breakers and arc fault circuit breakers (AFCB). The circuit breaker ratings were chosen using standard industry practice for the gauge of the test wire. Fuses were used in only a couple tests to limit the duration of any electrical activity.

A.1.4 TARGET GEOMETRY AND MATERIAL

The target geometry and material were selected from those found on aircraft that could cause problems if damaged. This included aluminum (6061-T6) and titanium (Ti-3AL-2.5V) tubes, steel flight control cables, aluminum spars as well as steel and aluminum rectangle of different thicknesses. As the arc damage model is being developed, it must correctly account for the different thermal properties of the target material. Similarly, the model must be able to account for different geometries.

A.1.5 WIRE GAUGE

In general, there is an increase in the amount of damage done by an arc as the conductor size increases. This is because:

- there are higher arcing currents (power) available,
- the circuit protection is rated at a higher level allowing the arc to continue longer before tripping,
- and the conductor does not erode away as quickly in the arc, allowing the arc to continue longer.

The range of wire gauges tested included 10, 14, 16, 20, and 24 AWG, which represent the span of gauges found on an aircraft excluding the large power feeders. Fault currents were consistent with those possible on an aircraft with unrealistic values excluded. (For example to limit the current in 16 gauge wire to 100 amps would require about 1.6 ohms of resistance or about 350 ft of 16 gauge wire, which is an unrealistic length for an aircraft wire).

Not all of the target geometries and material were used for each wire gauge. For the 24 AWG wire, the targets were limited to only aluminum hydraulic lines. Additionally, some of the larger gauge wires (10, 14, and 16 AWG), were only used on a select number of targets.

A.1.6 SOURCE VOLTAGE

The large majority of the testing used a source voltage of 115 VAC to ground, as the historical data indicates that more damage has been done at this voltage level. There was limited testing of 28 VDC circuits. Wet arcing was omitted from the 28 VDC testing because previous testing has shown that wet arcing does not occur in a 28 VDC circuit unless the salinity of the fluid is increased to 10%, which is unrealistic in an aircraft.

There were two different mixed power sources to be tested. The first configuration was a 115 VAC wire arcing to a 28 VDC wire. This was tested using the wet arc test initiation method with the configuration that produced the most damage during the baseline tests. The second configuration was a three-phase 115VAC test configuration. Two of the three phases were connected to active wires and was performed utilizing the wet arc test initiation method. The purpose of this tests was to show how different power source can effect the damage due to arcing, especially the higher voltage levels of the phase–to-phase arcing

A.1.7 SEGREGATION MATERIAL

The segregation materials tested were Teflon tape, Roundit 2000NX, and Silica/PFA. These tests were performed using the guillotine method with a grounded blade in which the active wire was not wrapped in the segregation materials but the passive wires were protected with the segregation material. Damage to the segregation material and passive wires were assessed using volume loss and dielectric voltage withstand tests. The voltage on the passive wires was monitored during these tests. Recorded damage was compared to similar guillotine tests done without segregation material.

A.1.8 WIRE SPECIFICATION

There were two ways that the insulating construction affected the damage caused by arcing. The first, the arc itself can be affected by the surrounding insulation. While a significant amount of energy can be released in any dry arcing, because it is primarily a metal-to-metal event, the surrounding insulation can tend to limit or increase the arcing intensity. The second effect is in the amount of damage done to the passive wires in the harness.

In one subset of tests, the active wire remained the same wire specification (81381) and different wire specifications were used for the passive wires. The primary aim of these tests was to measure the damage on the passive wires in the worst-case scenario.

The second subset of tests used different wire specification for the active wire as well as the passive wires. The aim of these tests was to measure differences in the arcing power dissipated and damage to targets and passive wire.

The specifications tested included those in common use on aircraft.

- AS22759/34 XL-ETFE: Cross-linked Tefzel
- BMS 13-60: Boeing Composite specification
- Airbus CF: Airbus polyimide with FEP topcoat
- Airbus DK: Airbus Composite
- Mil-W-81044/12: XL Polyalkene and XL Kynar (Poly-vinyldene Fluoride) used in Part 25 Business Jets and General Aviation

A.1.9 DIRT AND DEBRIS

The purpose of these tests was to determine if an arc could ignite dirt and debris on the harness adjacent to the arc site. Aircraft lint that was provided by the FAA Tech Center was used in these tests. The guillotine test was used for this test because the harness (and dirt and debris) was not subject to movement or moisture.

A.1.10 DAMAGE AT A DISTANCE FROM THE ARCING HARNESS

These tests used the wet initiation method with target wires placed at distances of between ¼" and 1" from the arcing harness. The loss of insulation from the target wire was measured in terms of volume loss and via DVW testing.

A.1.11 EXPOSURE TIME (CIRCUIT BREAKER) DAMAGE CURVE

These tests evaluated the effect of arc duration on arc damage in greater detail. Tests with the same configuration except for the circuit protection (rating and type) were performed to give a range of exposure times.

A.1.12 EFFECT OF FORCE BETWEEN HARNESS AND TARGET (VIBRATION TEST)

The goal of these tests was to develop a curve that shows how the arcing waveform (power dissipated) changes as the force between the harness and target was varied in vibration tests. The force was changed by adjusting the position of the harness holder and was measured using a spring scale.

4.2 INITIATION TEST METHODS DESCRIPTION

The following section describes the four arc initiation methods that were used in the testing phase of the project. These initiation methods include the swing, vibration, wet, and guillotine initiation methods. Some of these are based on existing industry specifications for arc testing, but were modified to accommodate the special needs and goals of the testing. A more detailed description of each test method is found in appendix A.

A.1.13 SWING TEST

The swing test represents a ticking fault situation where a metal to metal contact is made momentarily and then separation occurs: for example, when a swaying bundle abrades the wire insulation and then the connector touches structure. Figure 8 shows a diagram of the test apparatus.

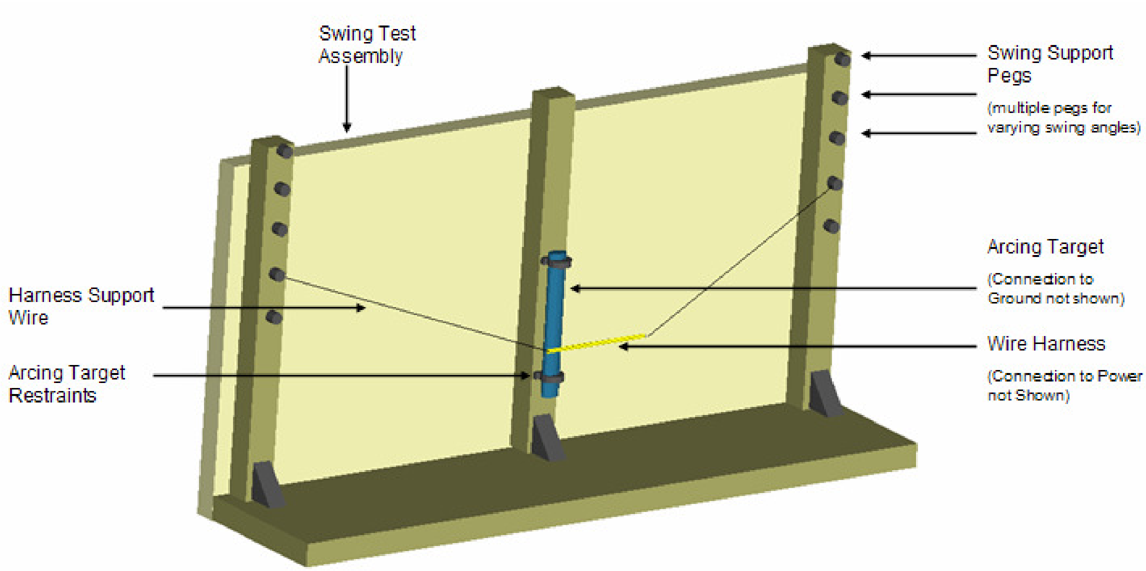

Figure 8. Diagram of swing test. Connection to power not shown.

The arcing targets used were aluminum or titanium tubes, steel fight control cables and aluminum structure (spar). Figure 9 shows a cross-section of the six-over-one 7-wire test harness. The active wire was pre-damaged and initiated the arc when it struck the target.

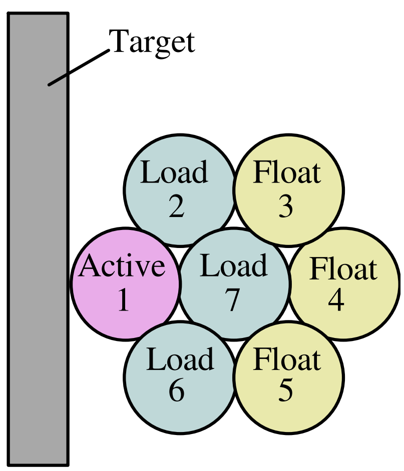

Figure 9. Cross-section of swing test harnesses.

The circuit diagram for the swing initiation method that used 115 VAC power can be seen in Figure 10. It shows the active wire connected to phase A of the generator through the circuit protection and the series resistance wire that determined the fault current. The target is grounded to the neutral of the generator. A simulated load (50 Ω) was connected to the passive, load wires. The test instrumentation is shown in blue.

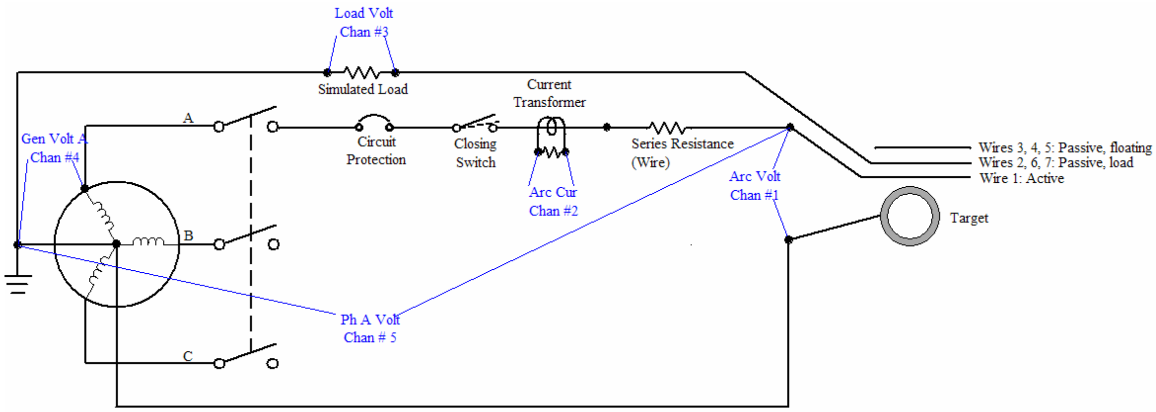

Figure 10. Circuit diagram for the swing arc initiation method with an 115VAC power source.

The circuit configuration of the other initiation methods described in this section is similar to that seen in Figure 10.

The main purpose of this test was to record the damage (mass removed) done to the active wire conductor and to the target. In addition, the damage done to the other wires in the test harness was measured. The swing test, together with the vibration test was used to generate the vast majority of the dry arcing data.

A.1.14 VIBRATION

The vibration test method represented the situation on the aircraft where a wire harness has come to lie on a metal piece of the aircraft. The wire then chafes through the insulation and arcs to the metal object due to vibration.

In the vibration test, an arc is created between a pre-damage wire on the outside of the test harness vibrating on a metallic target such as a hydraulic lines or flight control cables. Figure 11 shows a 3-D model of the test apparatus with the wire bundle crossing at a right angle with the target. The harness configuration and test circuit for the vibration test was identical to that of the swing test. For selected tests, a thermocouple was attached to the target near the arc location. Because of the slow response time of the thermocouple, the instantaneous temperature of the target during the arc can not be measured, but ultimate temperature of the target which is directly related to the total arc energy that entered the target can be measured.

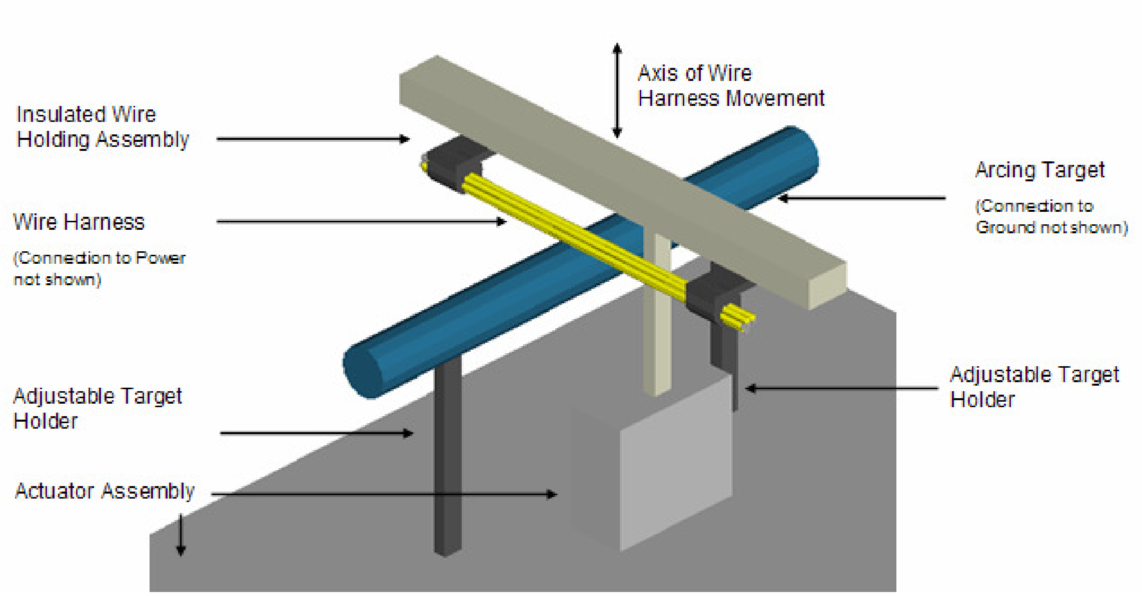

Figure 11. Diagram of vibration test stand. The electrical connections for the wire harness and the arcing target are not shown.

The main purpose of this test was to record the damage (mass removed) to the test wire conductor and to the target. In addition, the damage done to the other wires in the test harness was measured.

In shakedown tests, the consistency of the results was improved if some of the test parameters were controlled. These parameters include the frequency, displacement of the vibration, and the force between the bundle and target. For a majority of the tests, the maximum resting weight of the wires on the target (the pre-vibration weight of wires at the bottom of the sinusoidal motion) was set to be within 10% of 100g. A small number of tests were carried out to investigate the damage with a variation in the maximum resting weight.

A major cause of inconsistent results with respect to the vibration initiation method, had been found in variations at what point in the vibration cycle that the power was applied to the harness (e.g. is the conductor above the target, touching the target or just touching/moving away from the target). It was not possible with the configuration used to control power activation with this test method.

Because the movement of the test wire relative to the target was controlled fairly tightly, the volume of insulation removed from the wire was small so that the insulation is in close proximity to the arc and effects of the insulation on the arc could be measured.

A.1.15 <u>WET TEST</u>

The wet test represents a scenario in which fluid contamination creates an arc between two damaged wires (Figure 12). In general, the tests followed the AS4373 Method 509 procedures with appropriate modification where needed to meet the goals of this project. A target wire was placed above the test harness at a distance of ¼", ½", ¾", or 1 inch. Because this could interfere with the dripping of the saline (3%) solution on to the test harness the wet droplet was placed on the test harness using a syringe before power was applied.

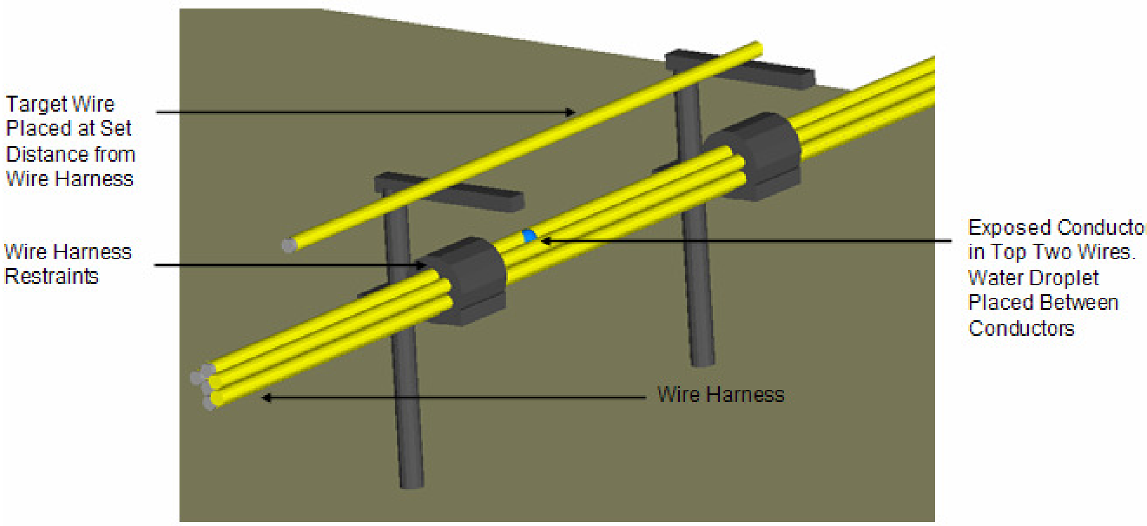

Figure 12. Wet test apparatus.

Figure 13 shows the circuit diagram for a phase-to-phase wet arc test. It is similar to the circuit for the swing test expect that there are two active wire that are pre-damaged.

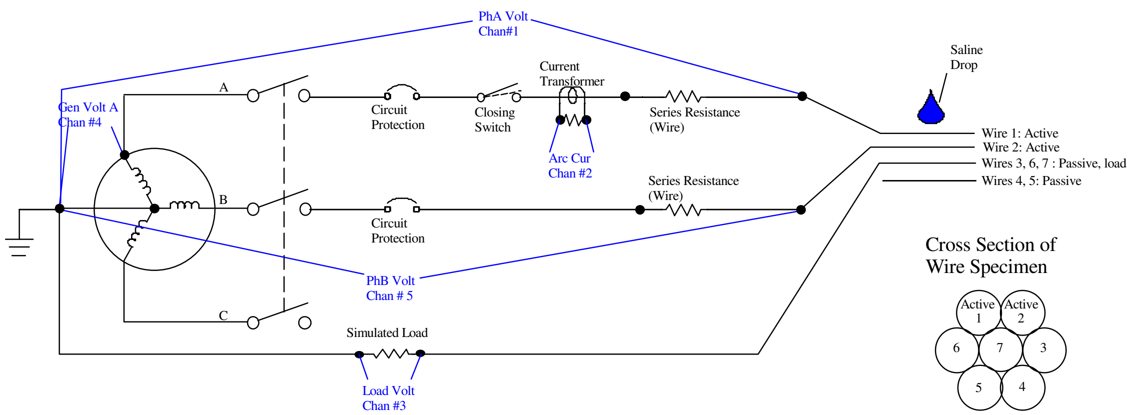

Figure 13. Circuit diagram for phase-to-phase wet arc test

The main goal of these tests was to gather data on damage to the passive wires in the harness and damage to objects at a distance from the harness. Additionally, a measurement of the plume temperature at a distance from the harness was investigated using this method. A novel technique that was used to measure the plume temperature was the Thermal Gradient Stratification technique (see damage assessment techniques). Also, in selected tests, a thermocouple was placed in an insulated tube (a 20 AWG wire with the conductor removed), placed adjacent to the target wire. This allows a measurement of the temperature of the insulation on the inside of the wire.

A.1.16 GUILLOTINE

The guillotine test followed the test method in AS5692 with modifications as needed to meet the goals of the project. One change was to use thicker “blades” in addition to razor blades. In these tests, aluminum rectangles that are 1/16” or 1/8” in thickness were used. The contact edge (the side making contact with the wire harness) of rectangles was not sharpened, so windows were cut into the active wire insulation to allow arc initiation. In some tests, the blade was grounded and only one of the wires in the test harness was damaged. The arc occurred between the blade and the active wire (blade grounded tests). In other tests, the blade was floating and the arc occurred when the blade bridged two pre-damaged wires in the test harness (blade floating test).

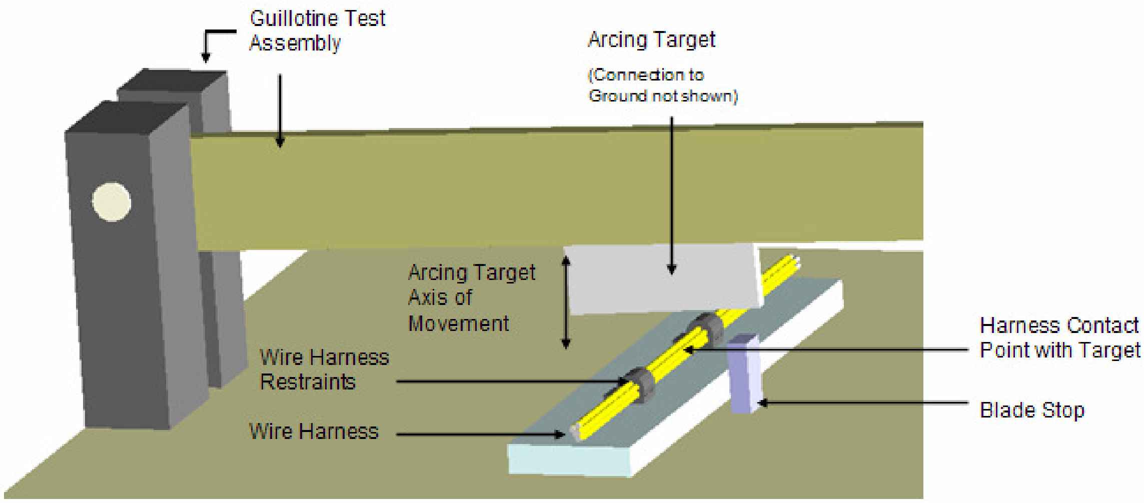

Figure 14. Guillotine test apparatus.

The main purpose of these tests was to measure damage to the target (blade) and the harness (passive wires). In a manner similar to the vibration tests, a thermocouple was attached to the blade near the arcing location; this was done in many of the guillotine tests. The blade grounded configuration was used in the segregation and the dirt and debris initiation tests.

4.3 DAMAGE QUANTIFICATION

This section describes in detail the type of damage to arcing targets and active/passive wires that were seen and the methodologies used in the arcing damage assessment. Five target geometries were used in the testing: pipes (aluminum and titanium), flight control cables, metallic blades, aircraft structures, and wires at a distance. Additionally, quantification was necessary for the wire bundles (both active and passive wires). For each of these, different methods were necessary to quantify the damage.

A.1.17 DAMAGE TO TARGETS

As part of the testing, each target was weighed (with the exception of the aircraft structure and wires at a distance) before and after each test to evaluate the amount of material lost as the result of the arcing experiment. It was the hope that this would provide information about of material lost from the target. After much experimentation however, weight loss was found not to be a good indicator of material loss or target damage. This was due in large part because copper from the active wire was added to the target obfuscated the material loss from the target due to arc damage.

One of the concepts repeatedly raised in damage quantification of the arcing target is *penetrating damage*. In many of the tests performed, there was surface scorching and target material loss as well as material transfer from the copper conductor to the target. *Penetrating damage* refers exclusively to the areas in the target where material has been lost.

4.3.1.1 BLADES

During guillotine tests, razor blades and aluminum blades (two thicknesses – 1/16" and 1/8") were used to initiate arcing. To quantify the damage done to these targets, the following methodologies were developed.

4.3.1.1.1 RAZOR BLADES

Stainless steel razor blades were used in 7 test groups, all using the guillotine initiation method. In most of these tests, the damage to the razor blade was penetrating with very little variation between the front and rear side damage of the blade. For the razor blade, a simple surface area measurement was made and multiplied by the blade thickness to gather the material lost information. The small variation in blade thickness at the cutting edge was ignored.

Figure 15. When razors were used as targets, the surface area damage was the nearly the same on both sides of the target (the razor blades were 10 mils thick). The figure above is representative of the damage from arcing to the razor blades. This photo is from TG-037-02. The scale in the photo is 1mm x 1mm.

Figure 15 is representative of the type of damage seen in the razor blade guillotine tests. The tests were performed with the intention of initiating the arc not immediately below center hole of the razor blade, but as seen in Figure 15, that was not always the case. In the tests where damage to the blade enveloped the center hole, the total area was measured, and the center hole area was removed from the measurement.

4.3.1.1.2 ALUMINUM BLADES

Aluminum blades were used in 64 test groups as the target during guillotine tests: 22 tests involved the 1/16" thick aluminum blade and 162 tests were performed with the 1/8" thick aluminum blade. Both blades thicknesses were made of the same 6061 aluminum alloy.

The method described for the razor blade could not be used in the aluminum blades damage assessments. The thicker aluminum blades had different levels of damage on the front and back of the blades (the front side of the blade used here meaning the side facing the incoming power in the test). Thus a single measurement to assess the damage to the aluminum blades was not possible.

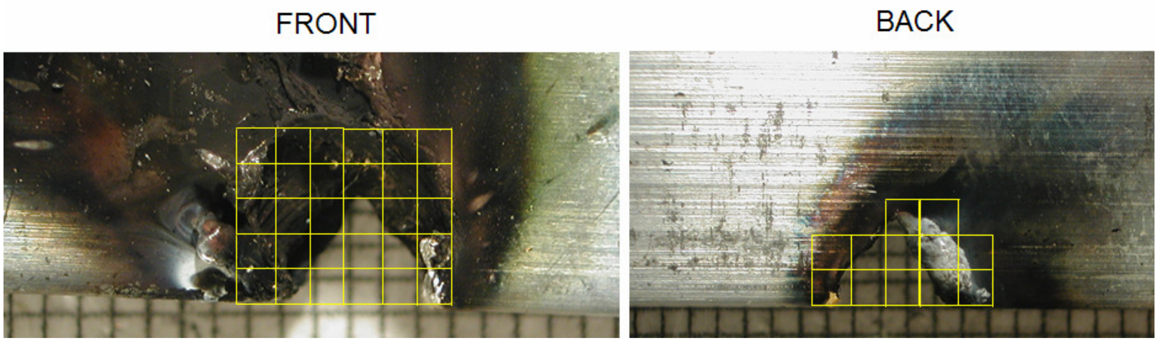

Figure 16. The yellow boxes in the above figure indicate one square millimeter of surface area that was damaged as a result of the arcing event. The front side the blade (left figure) has a significantly greater amount of surface damage than the back (right figure). The above figures are from TG-123-01. The scale in the photo is 1mm x 1mm.

As can be seen in Figure 16, the damage to the front and back of the same blade is significantly different, thus requiring a different methodology than the razor blades. The surface area on the front and back of the blade was measured, averaged, and then multiplied by the blade thickness. This calculation provided an easy and relatively accurate estimate of the amount of material lost.

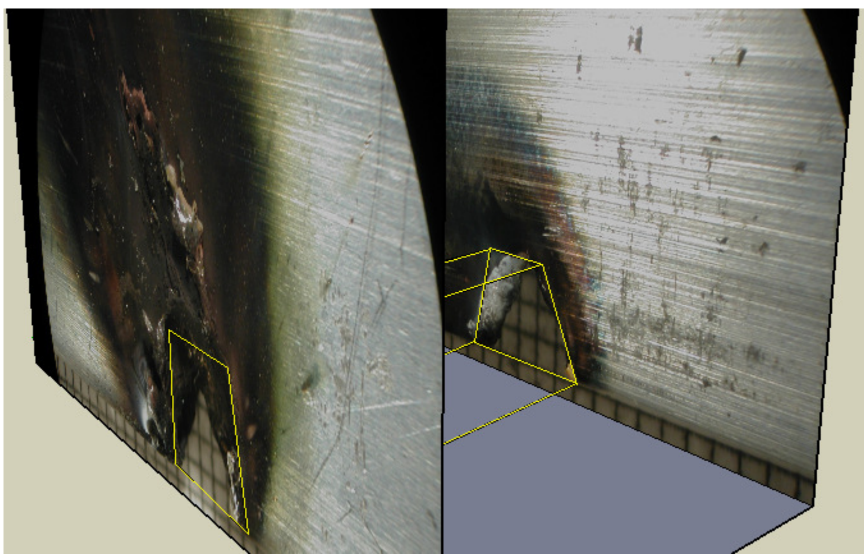

Figure 17. The above figure (same as those seen in Figure 16) shows the front and back sides of a damaged aluminum blade. The approximation of the damage area is done by averaging the area of damage on both sides and multiplying by the thickness of the blade. The estimated damage column is outlined with yellow polygons on the front and back of the blade. The scale in the photo is 1mm x 1mm.

A visual representation of this can be seen in Figure 17, the approximating volume lost outlined with the yellow polygon. This method was employed for both the 1/16" and 1/8" thickness blades. The calculation results are provided in the summary tables.

4.3.1.2 <u>FLIGHT CONTROL CABLES</u>

Flight control cables were used as the arcing target of swing/vibration tests in 13 test groups (52 tests total). The flight control cables that were used in testing were multi-strand cables in compliance with MIL-DTL-18375, "Wire Rope, Flexible, Corrosion-Resisting, Nonmagnetic, for Aircraft Control".

The flight control cable configuration can be seen in Figure 18; a 7x19 stranded core cables were used in all tests. The seven independent ropes within the flight control cable made it possible for an evaluation of each individual rope (see Figure 18).

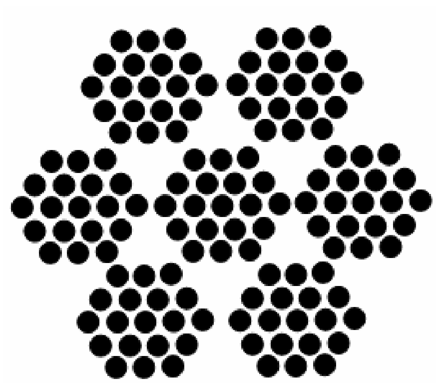

Figure 18. Configuration of the flight control cables that were used as targets during the testing. The six outer ropes are wrapped around the inner rope.

In testing, a number of strands from several individual ropes could be damaged or destroyed with a large amount of re-solidified steel spanning multiple ropes. Because the strength of the stainless steel flight control cables, good cross-section measurements of the cable could not be made. A representative example of damage to flight control cables can be seen in Figure 19.

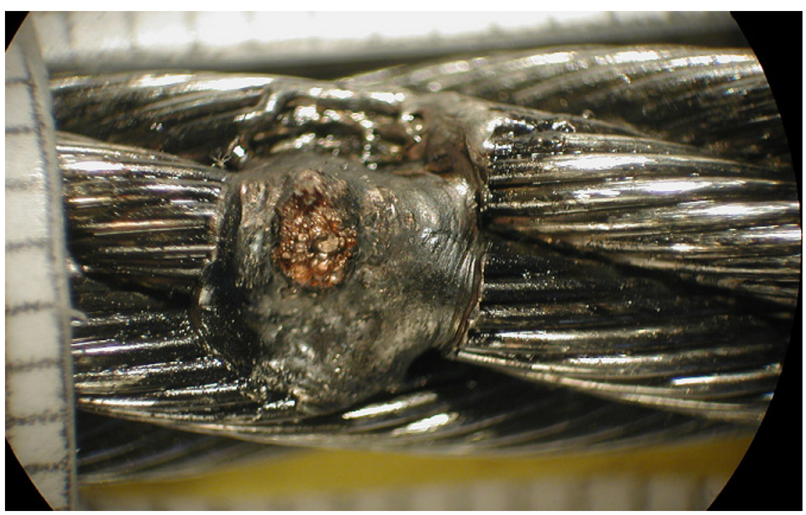

Figure 19. The flight control cable in the photo above had damage to three of the individual ropes, with significant damage to the rope in the middle of the photo. The amount of damage to the middle rope is obscured by the molten metal that solidified in the damage area. The above figure is from TG-073-01. The scale in the photo is 1mm x 1mm.

For evaluation of the damage, the individual ropes were unraveled from the flight control cable and each rope was evaluated and given one of five different ratings: 0-25% of the individual strands in a rope damaged, 25-50% of the individual strands in a rope damaged, 50-75% of the individual strands in a rope damaged, 75-100% of the individual strands in a rope damaged, and all strands damaged or destroyed (see Figure 20).

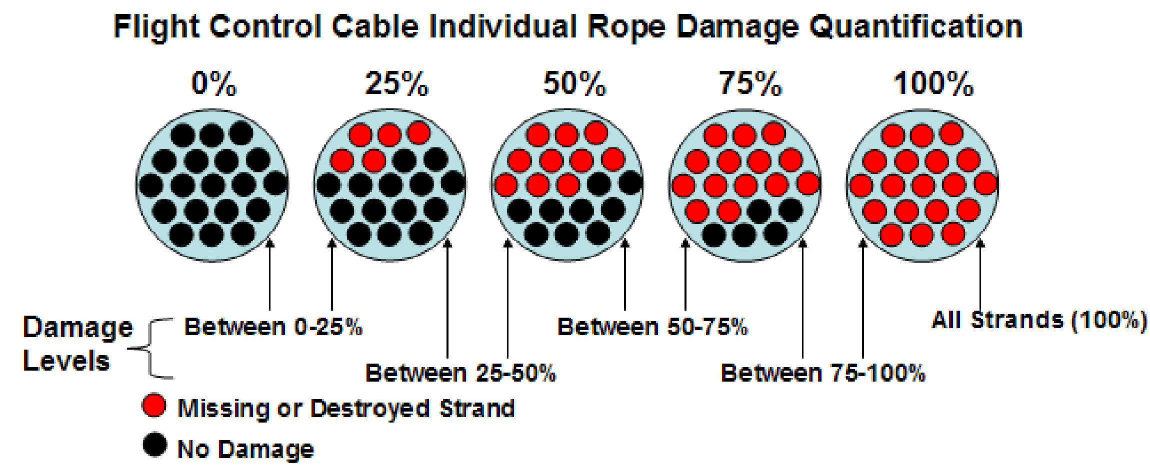

Figure 20. Flight Control Cable Individual Rope Damage Quantification.

The level of damage to each rope was estimated and the length of the damage was measured. Combining the results of all seven ropes provided an estimate as to the total amount of material damaged/lost. The overall flight control cable damage is reported in the test summary tables.

4.3.1.3 TITANIUM AND ALUMINUM TUBES

Hydraulic lines were used in 78 test groups as the target of swing/vibration tests: 260 tests involved the aluminum tubes and 52 tests were performed with the titanium tubes.

The hydraulic lines are of particular interest in the quantification methods. Because in practice these lines are pressurized, it is not necessary for the arcing damage to breach the tube; some penetrating damage can be sufficient to reduce the material strength to a point at which the internal pressure would cause the tube to rupture. As such, a more methodical approach was taken in the evaluation of damage to the hydraulic line targets than with the other targets in the testing. This was necessary as the thickness of the lines was as little as 26 milli-inches (0.66 millimeters).

Because penetrating damage to hydraulic lines and plates was difficult to measure visually, a precision depth measurement device was used, as seen in Figure 21. The depth gauge had an accuracy of (+/-) 0.001 inches, which was sufficient in the measurement of damage to targets.

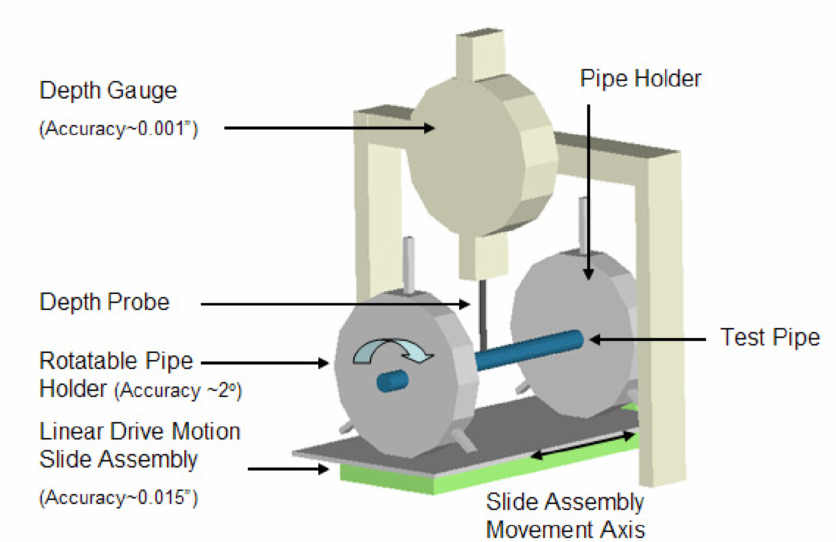

Figure 21. Diagram of method for evaluating the penetrating damage done to hydraulic lines and pipes during the arc damage experiments.

The depth of the damaged area was probed with a fine point needle; this made it easier to avoid measurement area averages that would come about with a larger probing device. Though there was some pressure on the depth gauge, excessive force was not applied to mitigate penetration into areas not damaged.

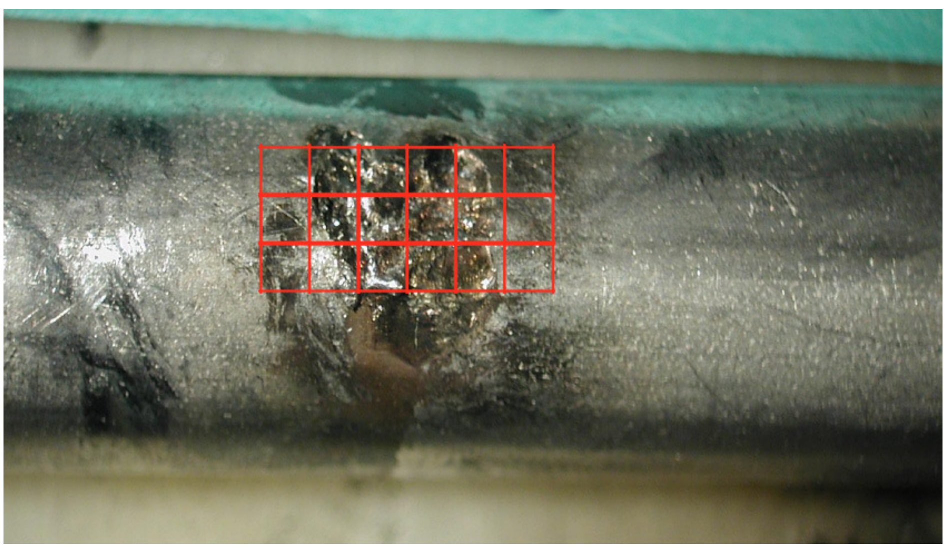

Figure 22. Photo of aluminum tube that has been damaged in an electrical arcing experiment. The red overlaid grid is an example of locations on the damaged pipe where depth measurements would be taken.

With the pipe fixed, the platform was moved back and forth to survey the damaged area of the pipe. An example of measurement locations can be seen in Figure 22; measurements were made 1mm apart in a grid pattern.

The data points gathered from the depth probe analysis were entered and linear interpolations were be made between the data points gathered. This was then translated into a 3-dimensional surface which was calculated and compared against an undamaged pipe for material loss estimates. An example of this can be seen in Figure 23.

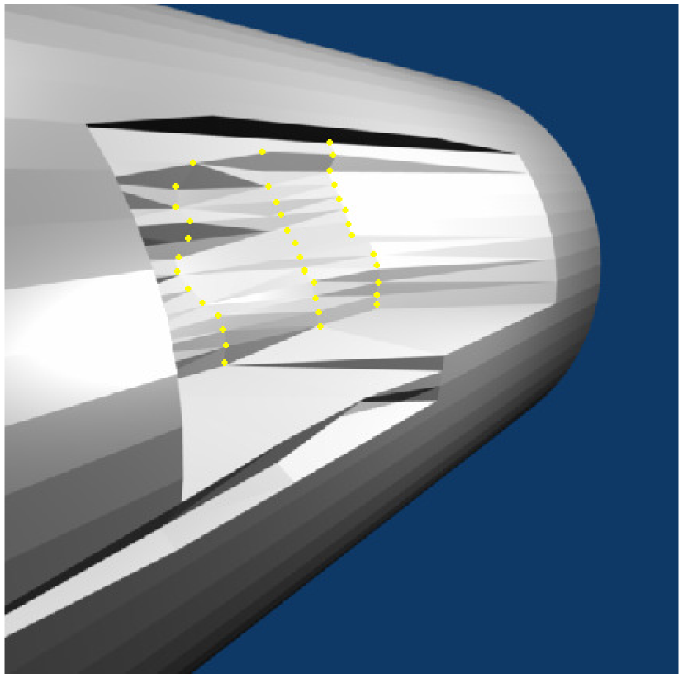

Figure 23. This figure shows the type of damage that was seen and could be represented with the depth probe measurements. Depth of damage exaggerated to show contrast between damaged and undamaged areas. Yellow dots indicate where probe measurements would have been made.

In the summary table, there are two values for the depth probe measurement: ‘Mass-Volume Loss’ and ‘Penetrating-Volume Loss’. The Mass-Volume Loss considers the total depth probe measurements which can include measurements that are above the surface of the tube. The Penetrating-Volume Loss ignores all measurements higher than the surface of the tube; this provides information for an estimate of material moved/destroyed in the tube. The results from the Mass-Volume calculations combined with the Penetrating-Volume calculations can show the amount of material that was displaced as the result of the arcing event. Depth probe measurements were not performed on those hydraulic lines where the arcing damage was negligible or created a hole in the tube.

4.3.1.4 STRUCTURE

Aircraft structure was the target in 11 test groups (33 tests total), with the swing initiation method used for all test groups. A representative example of damage can be seen in Figure 24; the damage to structure was typically about the length of the slit in the insulation of the active wire with scorching both above and below the target area.

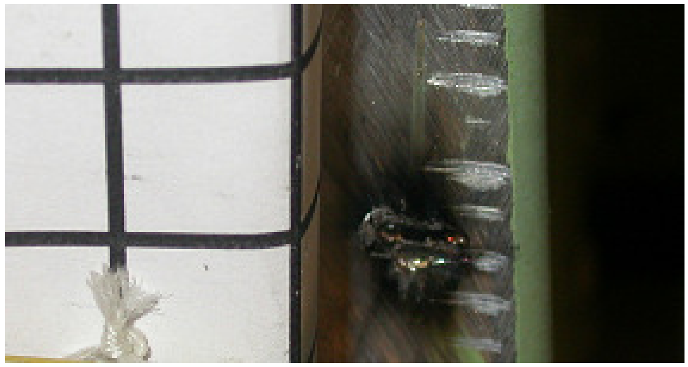

Figure 24. Damage to aircraft structure as the results of arcing. Some penetrating damage into the target, but there was no penetration of the structure. The above figure is from TG-018-01. The scale in the photo is 0.5 inch x 0.5 inch.

As can be seen in Figure 25, the wire bundle was setup such that the arcing would occur in the middle of the flat section. However, due to the variations in the swing test, the damage site was occasionally at the bend in the structure.

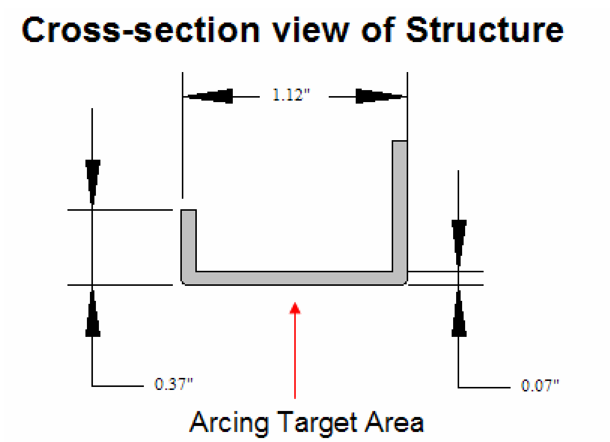

Figure 25. Cross-sectional diagram of structure. The wire bundle was setup such that the bare conductor would strike at the center of the 'Arcing Target Area' noted in the figure.

Because of the size of the target, weighing the target and depth probe measurements were not reasonable options. Two factors were considered in the quantification of structure damage: area of the damage, and penetration. The quantification of the area was done by measuring the surface area only where there was penetrating damage.

The measurement of the penetrating damage was performed with modified handheld calipers using a needle as a probe, much in the same way as the depth probe was used for hydraulic lines. Visual inspection of the arc damage site defined the area of greatest depth of penetration. This was then probed and measured until the greatest depth of penetration was found. To measure the depth, the modified calipers were moved to the undamaged structure in the immediate area, and the difference was recorded. Multiple measurements were made until the variation in the depth was less than ±5mils. Tests with penetration of the structure were not probed. It was up to the best judgment of the person reviewing the target damage as to the level of penetration. To remain consistent, only one person made the evaluations of the damage level. Periodic reviews were performed to ensure that the acceptability of the evaluations.

To estimate the total amount of material lost, the maximum depth was multiplied by the damage surface area and divided by two. The overall structure damage is reported in the test summary tables.

4.3.1.5 THERMAL GRADIENT STRATIFICATION (TGS)

The TGS target was used in 7 test groups (21 tests total), with the wet initiation method used for all test groups. As the arc plume enveloped the TGS wire strands, areas of the wires were damaged or destroyed. In some cases, long segments of wire strands were destroyed (an example of this can be seen in Figure 26), in others, only a small segment in the middle of a wire was lost.

Figure 26. The figure shows the damage to the lowest layer of the TGS with damage to the wire strand running parallel to the test wires at a distance of 0.25”. Though the other wires on the same layer appear unscathed, there is 18mm of conductor missing from the wire strand immediately above the initiation site. The above figure is from TG-113-02. The scale in the photo is 1mm x 1mm.

The TGS was aligned both parallel and perpendicular to the bundle orientation; no changes were necessary in the damage evaluation methodology. The wire strands were set into a rig with defined horizontal layers and vertical columns; the results of the testing were evaluated in this manner.

Each layer of the TGS was photographed and the lengths of the damaged strands were measured. Additionally, the relative positions of the damaged strands were recorded. The results reported are only for the first three layers of the TGS as no damage was seen in any test above the third layer (a distance of 0.75” from the active wire).

The results from the TGS quantification will allow for arc plume energy and direction estimates to be made; these will be investigated in later in the project.

4.3.1.6 WIRE AT A DISTANCE

Wire at a distance was the target in 30 test groups (90 tests total), with the wet initiation method used for all test groups. The 81381/12 specification wire was used in most tests as the target. The method used for quantification of damage to a wire at a distance was the same as that which was utilized for the passive wire assessment described later in the *Damage to Wires* section.

A.1.18 DAMAGE TO WIRES

Six types of wire insulations that were used in the course of testing: 81381, 81044, 22759, BMS1360, Airbus-DK, Airbus-CF. The damage quantification methods described here apply to all wire types. Though, because of the different initial conditions of the tests, active and passive wires are quantified differently. Those wires that were used as targets in the *Wire at a distance* arcing tests, were quantified using the passive wire damage methods.

4.3.1.7 ACTIVE WIRE CONDUCTOR LOSS ANALYSIS

For active wires, it was necessary that a small breach be made in the insulation to expose the conductor and make it possible to initiate an electrical arcing event. The insulation removed from the active wires was recorded; the removed insulation will be considered in the estimation of material damaged/destroyed by arcing.

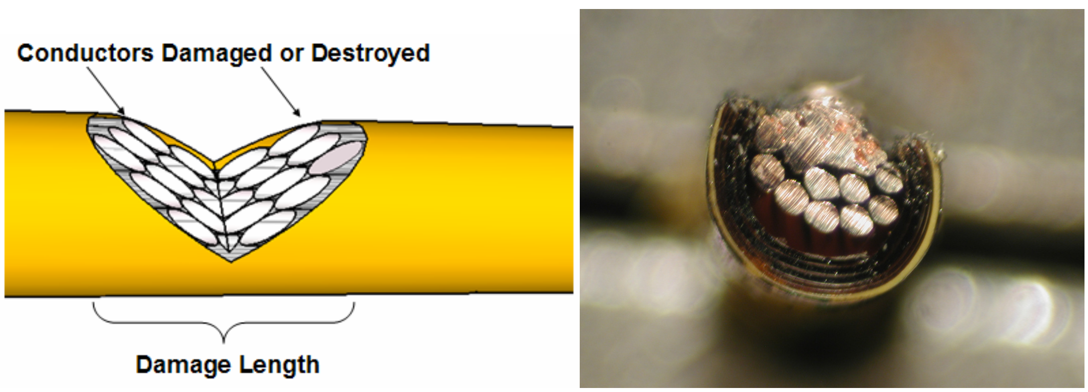

Figure 27. Diagram of active wire (left figure) showing typical damage profile seen in testing. For evaluation purposes, a cross-section cut would be made at the site (right figure) with the most damage, in this case at the center.

After the test, the active wire damage length was measured and recorded. A cross-section cut was then made through the wire at the location with the greatest number of conductors lost (If the wire was damaged sufficiently to sever the wire, no cross section photo was taken). The conductor strands were then counted, noting the number missing or destroyed. To calculate the amount of material lost, the following formula was used:

$$Mass\_Lost = \frac{Damage\_Length * \#\_Strands\_Lost * Mass\_Per\_Unit\_Length}{2}$$

This approximation assumes a damage profile similar to that seen in Figure 27, with a diminishing number of damaged strands near the ends of the damage area. An example of this can be seen in Figure 28 where there is an area of greater localized damage then progressively diminishes further away from the arc initiation site. Though the additional glob of metallic material seen in the figure is noted, it was ignored in the conductor mass loss calculation; in many cases it was too difficult to determine if the material came from the conductor or the target.

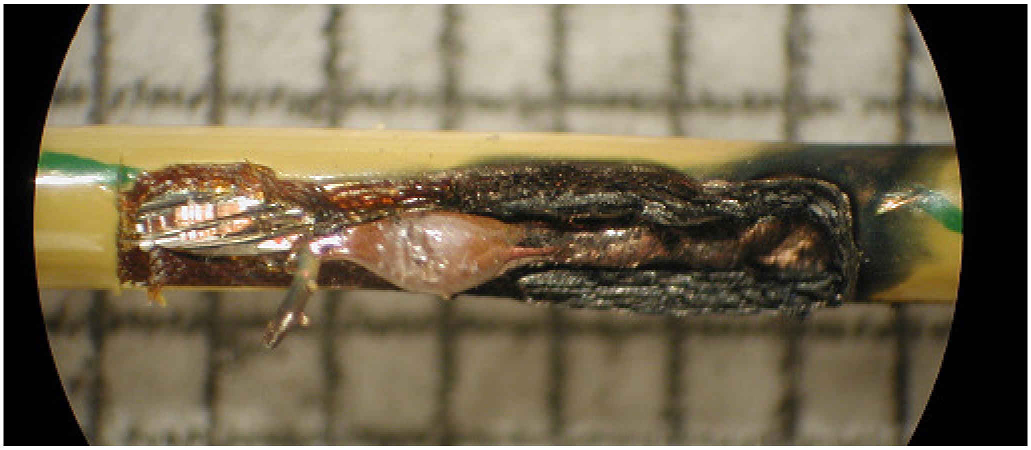

Figure 28. The damage to this wire is an example of the type of damage conductor damage seen. The above figure is from TG-141-02. The scale in the photo is 1mm x 1mm.

For initiation methods in which there were two active wires (wet test and non-grounded guillotine tests), both active wires conductor losses were measured in the same way.

4.3.1.8 PASSIVE WIRES

With the passive wires (those wires that were part of the test wire bundle in direct contact with the active wire), a similar method to the active wire damage quantification was employed. However, because the passive wires did not have initial breaches in the insulation, insulation damage quantification methods were necessary.

Unlike the wrapped insulations where layers of penetration could be counted when damaged, the level of penetration to the extruded insulated materials was difficult to assess. Cross-section analysis of the damaged areas in the extruded insulations distorted the insulation and made lost material evaluation difficult to accomplish. Because of this variation in wire insulation constructions, a single universal damage level measurement was used for all specifications. From this, meaningful comparisons of damage could be made between different wire types.

The scale of wire damage ranged from no wire damage to damage to the conductor. The damage scale runs from zero to eight, with a value of 0-8 possible for passive wires and 0-8 (with the exception of #6) for wires at a distance. The full scale can be seen in Table 2.

Table 2. Breakdown of the scale used to quantify damage to passive wires.

Damage Scale	Description
0	No Damage: Any soot marks on wire will rub off
1	Damage to Topcoat or Superficial damage to surface of insulation if wire doesn't have topcoat.
2	More than superficial but less than 50% of insulation thickness is damaged (missing). Passes Wet DVW
3	More than 50% of insulation thickness is damaged (missing) but the conductor is not exposed. Passes Wet DVW

4	Wire fails Wet DWV but conductor is not visibly exposed even under magnification
5	Conductor is visibly exposed
6	There was a load voltage measured during the arc (passive wires only)
7	The conductor was visibly damaged (passive or target wire)
8	A section of the conductor was missing (passive or target wire)

For all passive wire specifications, breaches to the conductor were evaluated in the same was as active wires.

4.3.1.9 WET DIELECTRIC VOLTAGE WITHSTAND TEST

If significant damage has occurred to the passive wires (as defined by the wire specification specific quantification methods) but the conductor was not visible, a wet dielectric voltage withstand test was performed. The wire was submerged in water and a 1500 VAC potential was placed on the conductor for 60 seconds to probe for breaches in the insulation.

A.1.19 ADDITIONAL QUANTIFICATION METHODS UTILIZED

In addition to the direct measurements of damage to the target and wires, additional quantification methods were used to gather information about the arc energy and thermal dissipation in the target.

4.3.1.10 THERMOCOUPLE ON TARGET

To gauge the thermal dissipation of energy through the target, a thermocouple was place on the target in some test configurations. Because of the irregular location of the arc in swing tests, it was impractical to place a thermocouple in these tests. The main use of the temperature measurement was in guillotine and vibration tests; the thermocouples were typically placed within 1-2cm of the initiation site. Additionally, in several of the wet tests, a thermocouple was placed inside of wire insulation sleeve taken from a striped wire. This was then run parallel with the target wire in the wet test to record the temperature rise in the area near the target wire. An example of this can be seen in Figure 29.

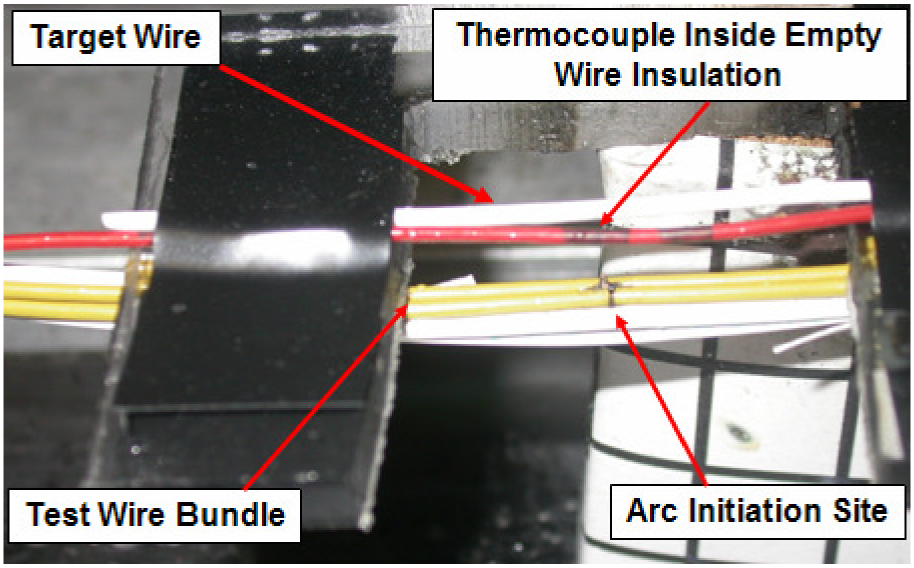

Figure 29. This photo shows the location of the thermocouple when used in wet tests. The 81381 type insulation was used to protect the thermocouple in all wet test, regardless of the specification of the target wire.

The distance from the expected arc initiation site was measured and photographed after the test was completed.

4.3.1.11 PHOTO SENSOR

As a means of gathering radiation from arcing, a photo sensor was placed a set distance from the arc initiation site and the voltage (related to the incident radiation) was recorded.
The purpose of this was to gather data on the amount of energy irradiated by the arcing event. Though it is not expected that a large percentage of the arc energy is converted to radiation, this photo sensor data will aid in the partitioning of the arc energy.

4.4 SAMPLE OF DATA ANALYSIS

During the performance of the 719 tests in the test catalog, a large amount of current and voltage data was collected as well as subsequent damage evaluation data. Figure 30 is an example of the voltage and current (V & I) chart in the excel spreadsheet. The blue curve is the arc voltage and the red curve is the arc current. This chart is from test TG-002-05, which was a swing test against an aluminum tube. In this test, there was an initial strike and then a second rebound strike before the circuit breaker tripped.

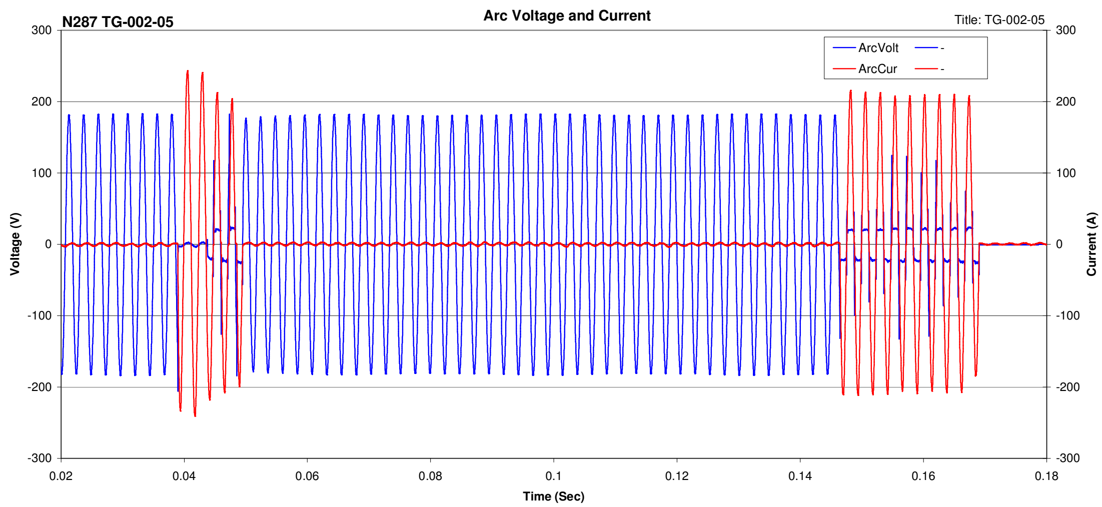

Figure 30. Arc voltage (blue) and current (red) in test TG-002-05.

Figure 31 is an example of the Power and Energy (P & E) chart in the excel spreadsheet. The purple curve is the arc power and the heavier black curve is the accumulated energy. This chart is also from test TG-002-05. The power data can be used as input data when testing the damage simulation models to be developed later in the project.

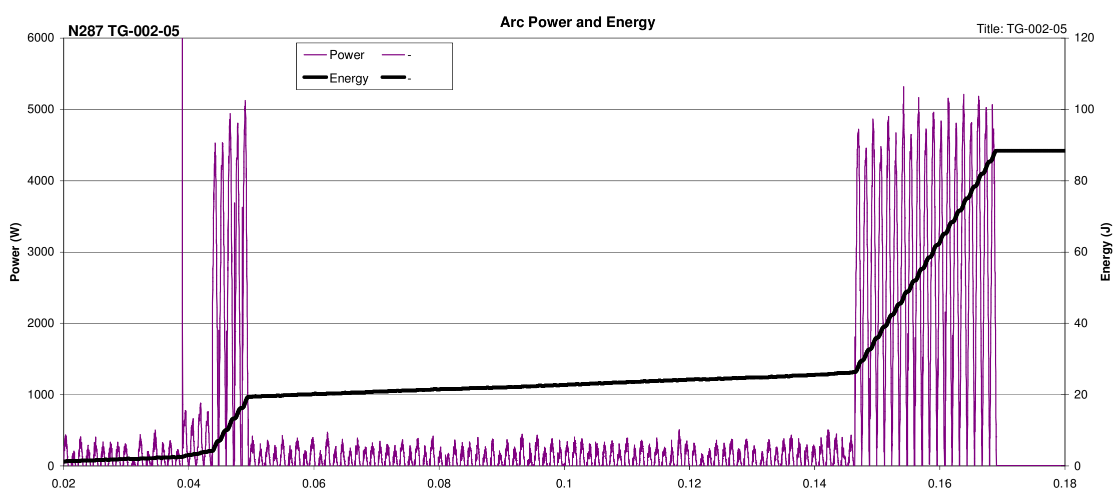

Figure 31. The power (purple) and accumulated energy (black) in test TG-002-05

Figure 32 is an example of the "Load" chart in the excel spreadsheet. The pink curve is the voltage measured across the load attached to the passive wires. The blue curve shows the arc voltage and is used for a frame of reference. This chart is from test TG-067-01 and it shows that after the 1.47 second mark, voltage was measured on the load. This means that significant power had been transferred from the arc into the circuit of the passive wires.

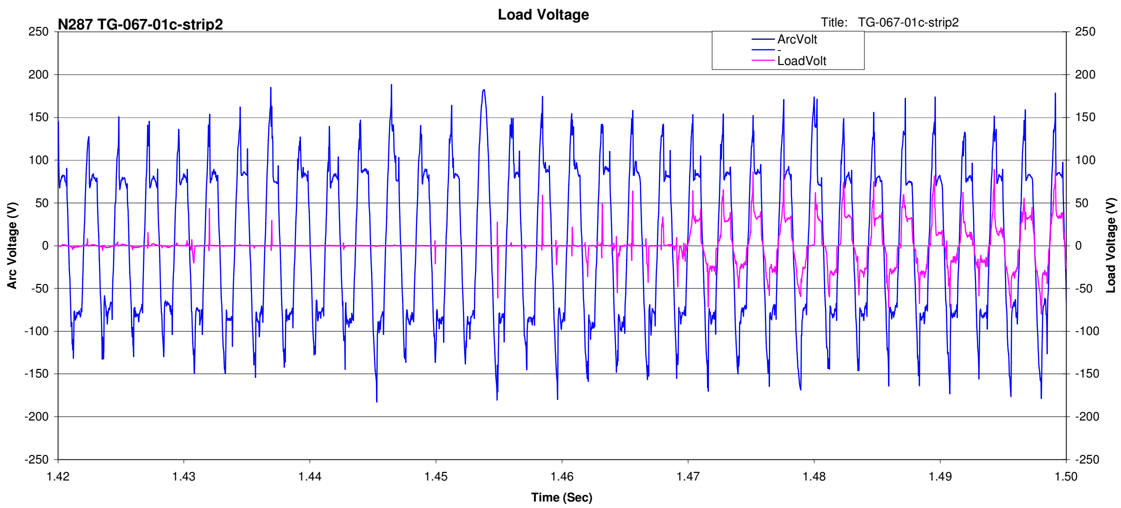

Figure 32. The load voltage (pink) with the arc voltage (blue) in test TG-067-01.

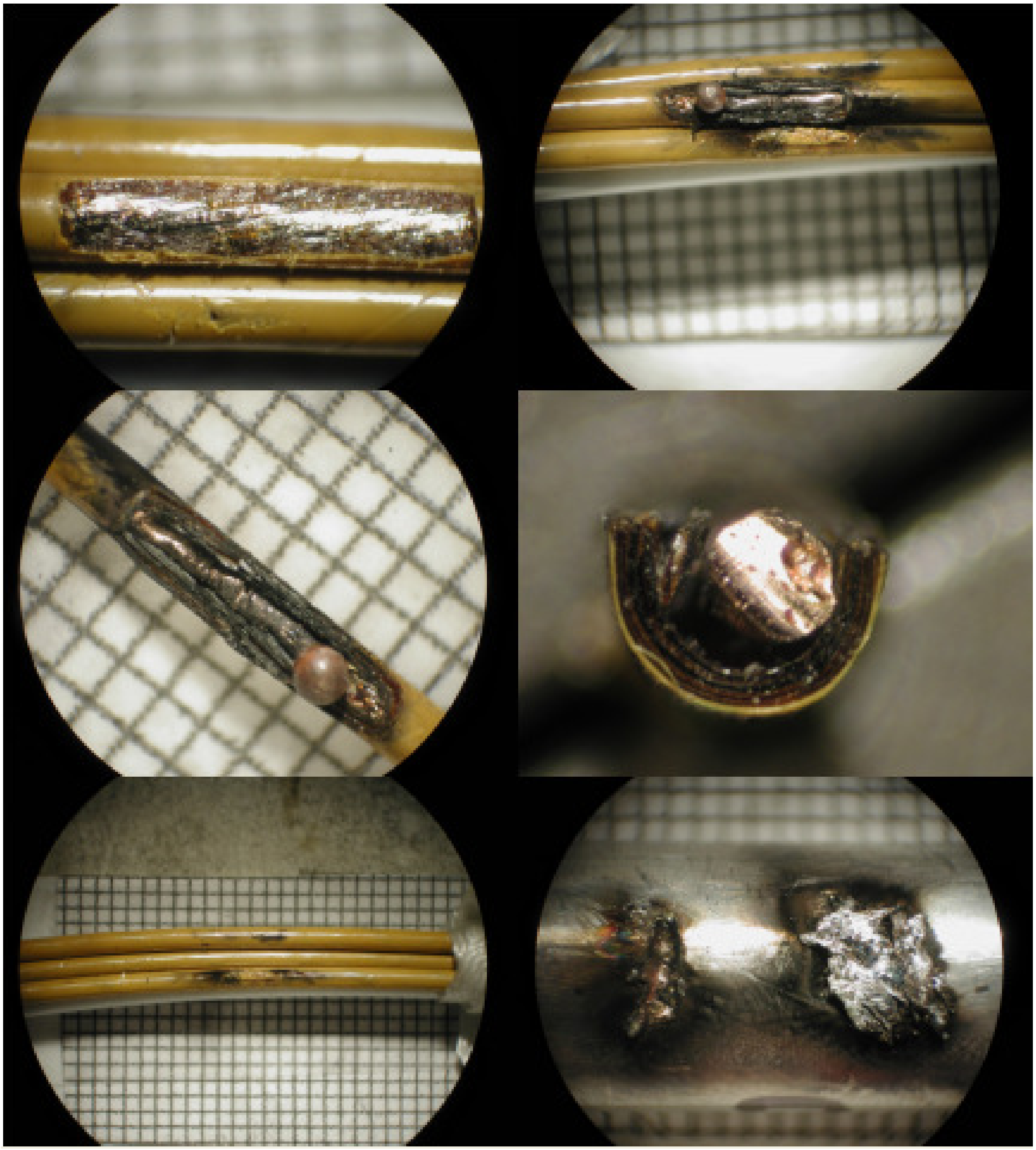

Figure 33. Examples of photomicrographs used to aid in damage quantification from test TG-002-05.

Figure 33 shows examples of photomicrographs that are available in the test folders.

- Upper left: Pretest of the test harness
- Upper right: Post-test of the test harness
- Middle left: Post-test of active wire
- Middle right: Post-test of active wire cross-section
- Lower left: Post-test of passive wires
- Lower right: Post-test of target

There is usually more than one photo of the damage to the target or test harness. If the damage to the active wire conductor was either superficial or extensive, then cross-sections were not made.

4.5 INITIAL ANALYSIS OF ARC DATA

Analysis of the arcing and shorting characteristics of the test waveforms need to be done quantitatively to build the model of arcing in later in the project. To expedite this task, a program was written that evaluated the text file conversions of the Nicolet files. The program used the arc voltage zero-crossing to divide the data into intervals. It then evaluated the interval using the duration, current and voltage levels and classified the interval as to whether it was a arcing, shorting, combination, or open ½ cycle, or if it was noise (contactor closing etc.). If it was an arcing or shorting ½ cycle, the peak and RMS current, arc voltage, peak power and energy dissipated in the ½ cycle was calculated. Using this program, all the test waveforms were evaluated in a batch mode. This included over 35,000 arcing and 13,000 shorting ½ cycles. This data was stored in a spreadsheet with the test parameter data.

Figure 34 shows the normalized distribution of the accumulated energy in the arcing ½ cycle for different fault currents. This includes all single phase test data including different initiation methods (i.e. swing, vibration, guillotine and wet), targets, active wire specifications and gauges etc. These distributions may become narrower when they are separated using these variables. Not surprisingly, it shows that fault current is a predominate factor in determining the energy dissipated in an arcing ½ cycle.

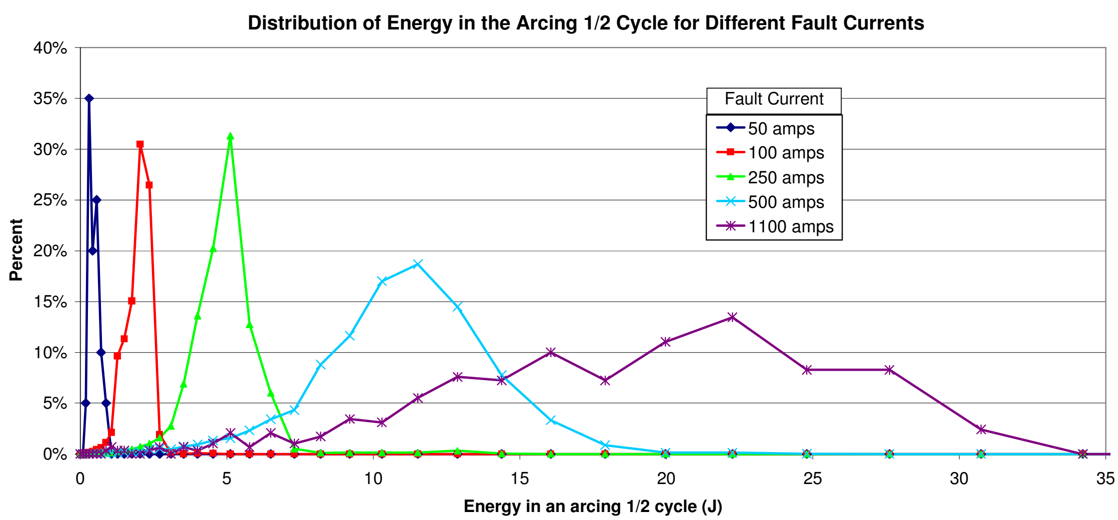

Figure 34. Normalized distribution of energy of the arcing 1/2 cycle of different fault currents

Figure 35 shows the average energy in a arcing ½ cycle as a function of fault current. The error bars represent one standard deviation in the data. Like Figure 34 it shows an increasing energy with fault current.

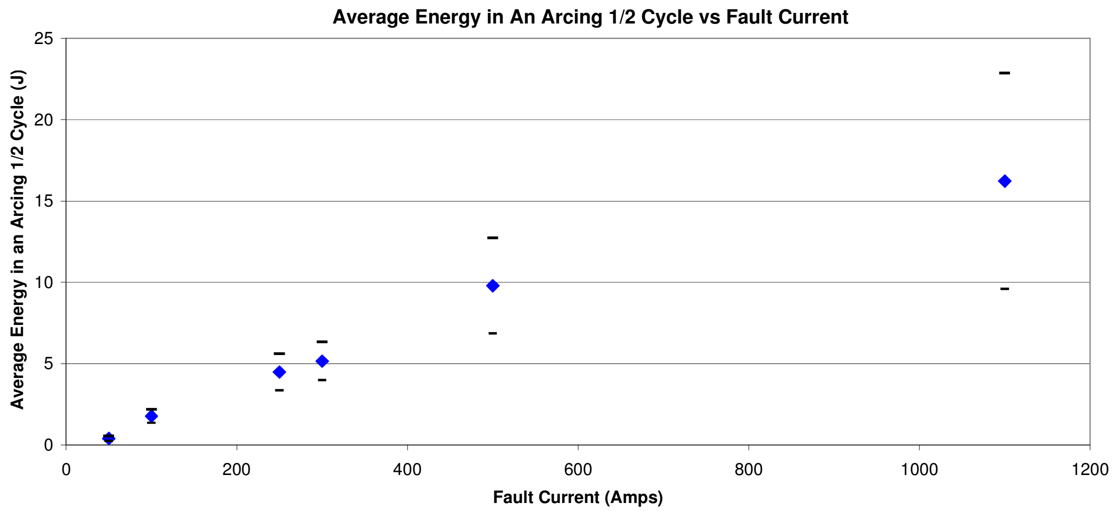

Figure 35. Average energy in an arcing ½ cycle as a function of fault current.

4.5.1 ANALYSIS OF SWING/VIBRATION TEST USING ALUMINUM OR TITANIUM TUBE

Initial analysis of the data in the test summary spreadsheets was done to examine trends in the data. Using the Swing/Vibration Aluminum Tube spreadsheet, the following was found:

- correlation between arc energy and volume damage to the target was 0.85,
- correlation between arc energy and volume damage to the active wire was 0.95,
- correlation between arc energy and damage index to the passive wires was 0.71.

These results are not unexpected and simply show that, in general, the more energy dissipated in the arc the more damage is done by the arc.

Measuring the amount of damage to an Al or Ti tube can be complex with the possibility of re-solidification of melted material and the possible addition of copper from the active wires. However, the penetration of the tube is a benchmark that is relatively easy to determine and indicates significant damage. The following analysis/conclusions were made using tube penetration as the damage criteria. The model created during the analytical stage of the project should be able to reproduce these trends.

4.5.1.1 ANALYSIS OF 115 VAC RESULTS TO ALUMINUM TUBE

The aluminum tube was penetrated on 49 of the 206 tests (24 %). The fault current is an important factor in determining the level of damage to the tube. Table 3 shows the number of penetrations broken-down by the fault current for polyimide insulated (Mil-W-81381) 20 AWG active wire. It shows that for 100 amps fault current, penetrations did not occur but raising the fault current to 250 amps caused a large number of tube penetrations. 250 amps had the highest percentage of penetrations as it seemed that the current level was high enough to deliver enough energy to damage to tube but low enough so that the circuit protection did not trip immediately. Note that the data in Table 3 is from tests using both thermal and arc fault circuit breaker

Table 3. Breakdown of the number of penetrations of Al tube by fault current (active wire was PI-20).

Fault Current	# Tests	# Penetrations	Percentage
100	8	0	0%
250	28	13	46%
500	9	2	22%
1100	3	1	33%
Total	**48**	**16**	**33%**

Table 4 shows the breakdown of penetration by the insulation type of the active wire. It shows that arcing with wires that have insulation systems that contain no polyimide (XL-EFTE and XL-PA {Polyalkene/Kynar}) cause less damage than those that do. Note that these results are for 20 gauge wire. For large gauge wires (16, 14) all of the wire types caused penetration of the tubes.

Table 4. Breakdown of the number of penetrations of Al tube by active wire type.

Insulation Type	# Tests	# Penetrations	Percentage
PI-20	48	16	33%
CF-20	16	8	50%
BMS1360-20	24	8	33%
DK-20	18	5	28%
XL-ETFE-20	25	1	4%
XL-PA-20	16	0	0%
Total	**147**	**38**	**26%**

4.5.1.2 ANALYSIS OF 115 VAC RESULTS TO TITANIUM TUBE

The titanium tube was penetrated on 20 of 53 tests (38%). All of these tests were done using Mil-W-81381 wire (20 and 14 AWG). Table 5 shows the number of penetration of the titanium tube broken-down by fault current. It follows a similar trend as the results from the aluminum tube with 250 amps having a high percentage of penetrations. However, in this case the 100 amp fault current did have penetrations.

Table 5. Breakdown of the number of penetrations of Ti tube by fault current (active wire was PI-20 and PI-14)

Fault Current	# Tests	# Penetrations	Percentage
100	7	2	29%
250	19	8	42%
500	17	5	29%
1100	10	5	50%
Total	**53**	**20**	**38%**

4.5.1.3 ANALYSIS OF THERMAL VERSUS ARC FAULT CIRCUIT BREAKERS

Table 6 shows the breakdown of penetrations by the type of circuit breaker: thermal or arc fault. It shows that there is a significant reduction of damage when arc fault protection is used. However, penetration of the tube can sometimes occur when using arc fault circuit breakers. Note this table contains data from thermal and arc fault breaker rated 5, 7.5, 15, 20 amps and each rating had at least one incident of penetration.

Table 6. Breakdown of the number of penetrations of Al and Ti tube by thermal and arc fault protection.

Circuit Breaker Type	# Tests	# Penetrations	Percentage
Thermal	156	61	39%
Arc Fault	95	8	8%

4.5.1.4 ANALYSIS OF 28 VDC RESULTS

The 28 VDC test were done using the swing or vibration initiation methods using a 3/8" aluminum tube target. In 42 tests, the tube was penetrated 19 times (45%). Further breakdown of the data, Table 7, shows that a large majority of the penetrations occurred when there were larger wire gauges and higher fault currents.

Table 7. Breakdown of 28 VDC test data by wire gauge and fault current.

Wire Gauge	# Tests	# Penetrations	Percentage
20	17	3	18%
14,10	25	16	64%
Total	**42**	**19**	**45%**

Fault Current	# Tests	# Penetrations	Percentage
25-50	13	0	0%
200-300	9	3	33%
400-600	20	16	80%
Total	**42**	**19**	**45%**

4.5.2 ANALYSIS OF DAMAGE AT A DISTANCE

Figure 36 shows the amount of damage done to target wires as a function of energy dissipated in the arcing event. The damage scale represents the damage to the target wire (0-8) and a short explanation of the level is shown on the graph. The figure contains data from both single and 3-phase wet arcing tests. The active wires were 20, 14 and 10 gauge polyimide. The target wires were 20 gauge polyimide, XL-ETFE or BMS-1360 wires and were at a distance of 0.25 inches above the active wires. The type of target wire insulation did not have a pronounce effect on the damage level. The fault current, wire gauge and circuit protection had a large effect on resulting arc energy and damage.

The results show that while there is large scatter in the data, there is a definite trend that higher energy levels will cause more damage to the target wire. This scatter is not unexpected because of the random nature of the arc. In some tests, the arc plume is deflected to one side and the target wire is not in the hottest part of the plume. However, even with the scatter, there appears to minimum energies needed to cause different levels of damage to the target wire. For example, to do more than superficial damage to the primary insulation (or topcoat), the arc needs to dissipate approximately 100 J or more. To damage the insulation such that the conductor is exposed requires 1000 J or more. Because arc fault circuit breakers limit the arc energy they also limit the damage to targets at a distance.

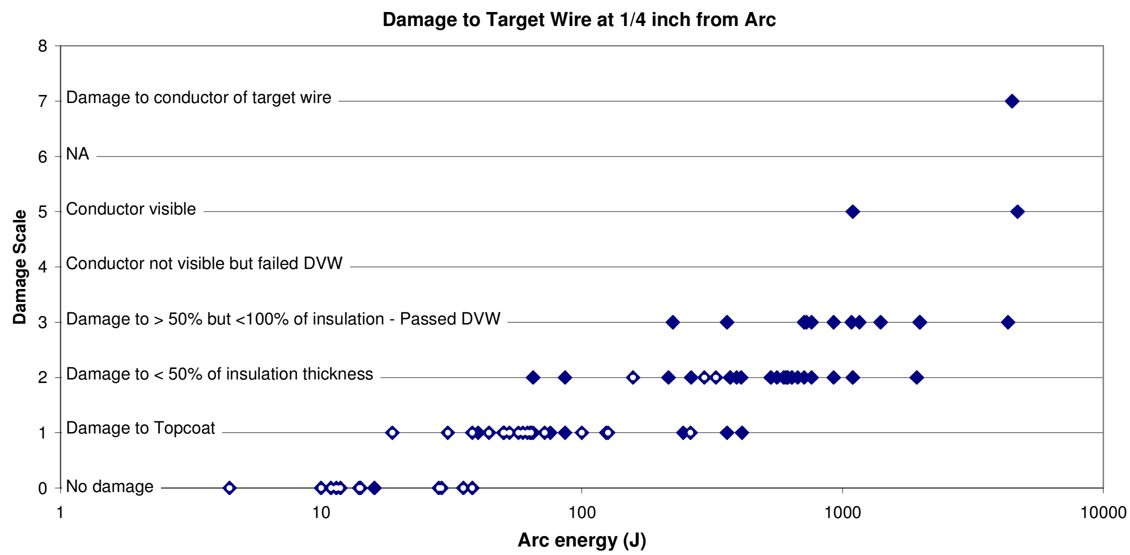

Figure 36. Damage to target wire for different arc energies (Diamonds with white spots indicate tests using arc fault circuit breakers).

The effect of the distance above the arc on the damage done to the target wire is shown in Figure 37. These are the average of results for arcing with 20 AWG polyimide active wires and 500 amp fault currents. There is significant damage to the primary insulation at 0.25 inches with an average of 50% or more of the insulation removed. However, at the 0.75 – 1.0 inch distance the damage is limited to the top coat or slight damage to the primary insulation. Even with the same test parameters the energy in the arcs varied from test to test. However, these results are from arcs that all had accumulated energy between 650 and 915 J.

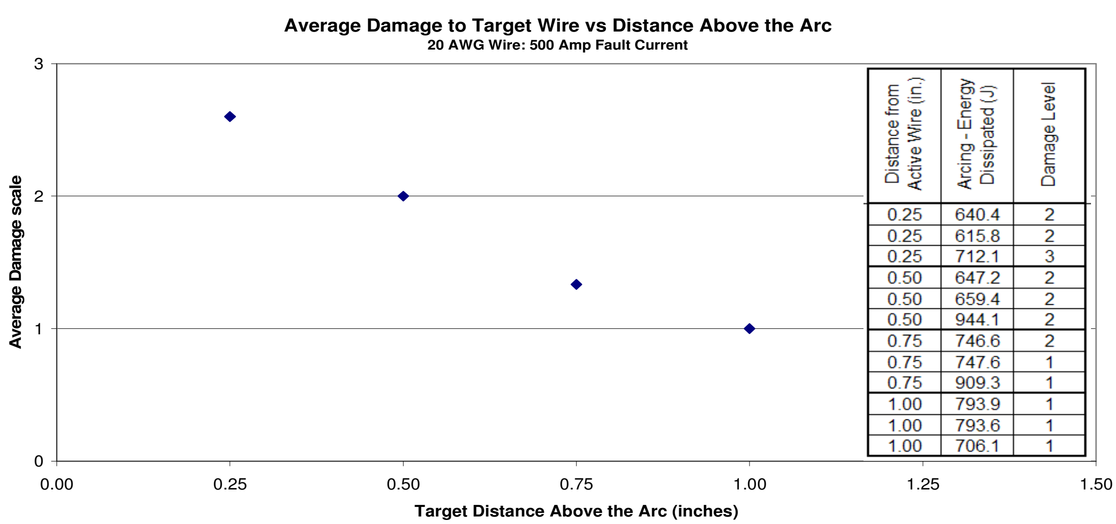

Distance from Active Wire (in.)	Arcing - Energy Dissipated (J)	Damage Level
0.25	640.4	2
0.25	615.8	2
0.25	712.1	3
0.50	647.2	2
0.50	659.4	2
0.50	944.1	2
0.75	746.6	2
0.75	747.6	1
0.75	909.3	1
1.00	793.9	1
1.00	793.6	1
1.00	706.1	1

Figure 37. Average damage to target vs. distance above arc.

Figure 38 shows a plot of the highest row of target small gauge wire damage during the Thermal Gradient Stratification tests. These results confirm the previous tests, that for arcing which dissipates less than 1000 J of energy, significant damage is generally done to a distance of ~0.5 inches above the arc. However, in one test in this energy range, damage was done to 4mm of one target wire at the 0.75 inch level. At higher energy levels, damage at greater distances is possible. At energies less than 200 J, damage at distances greater than 0.25 inches is unlikely.

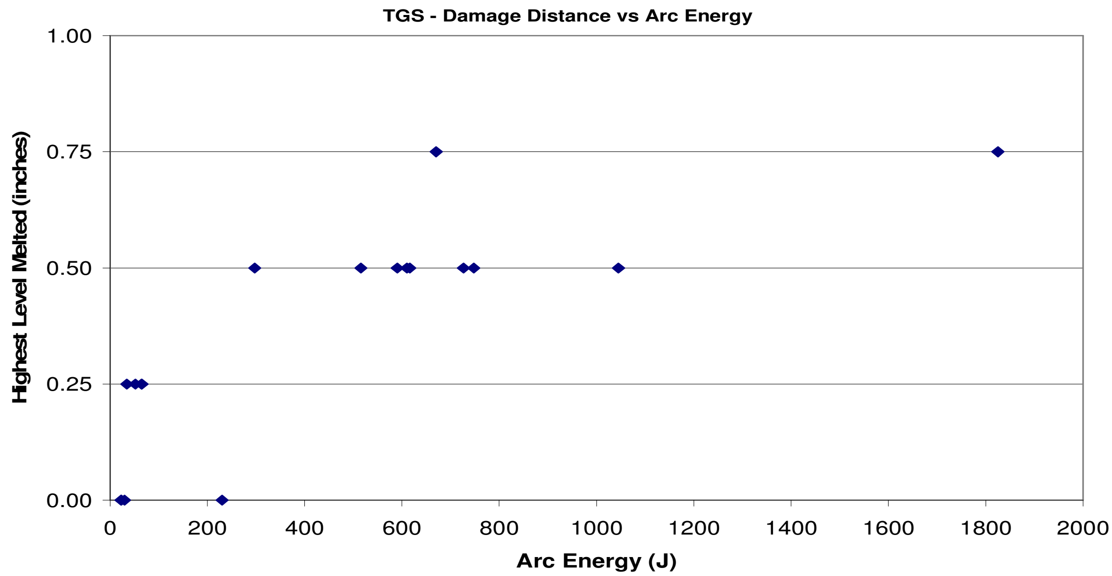

Figure 38. Results from the Thermal Gradient Stratification test

The fine wire matrix of the TGS setup did show that the shape and size of the arc plume did change from test to test. Of the 21 TGS tests performed, 13 of the tests were aligned so that the target wires perpendicular to the test wire bundle. The locations of the wire strand with respect to the arcing wires can be seen in Figure 39.

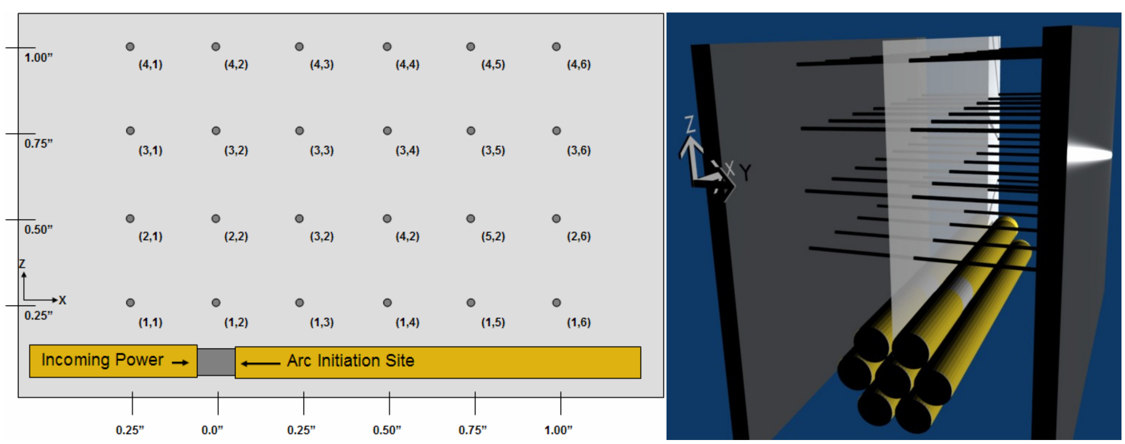

Figure 39. The figure on the left shows the layout and positions of TGS wire strands when setup perpendicular to the test wire bundle. The figure on the right shows which plane the data from which the following analysis is taken.

Figure 40 is a bubble chart of the spatial distribution of damage of these tests. The chart is oriented such that the incoming power to the test wire bundle was from the left.

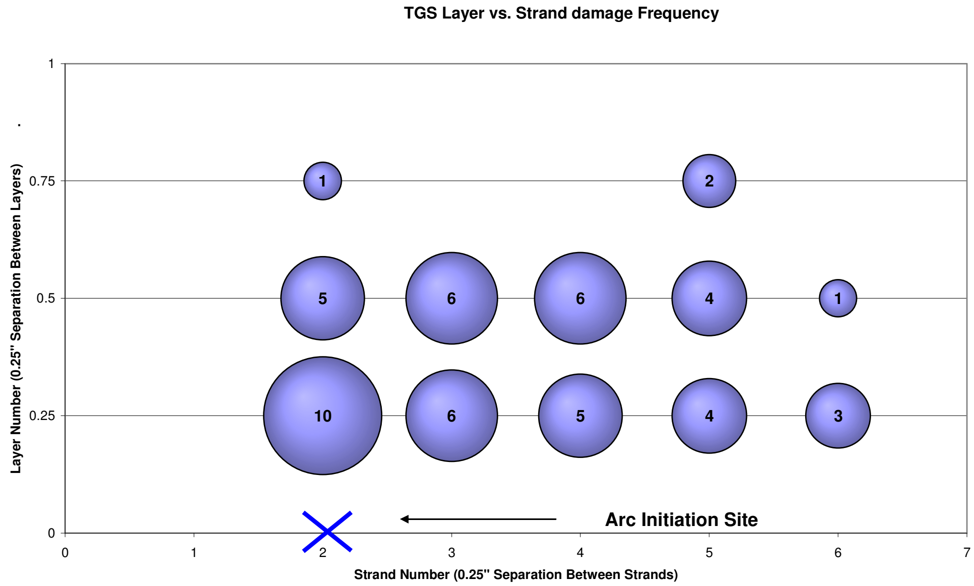

Figure 40. Bubble chart showing spatial distribution of damage for TGS tests in which the wire mesh was aligned perpendicular to the test wire bundle.

The number and size of the bubble represents the tests in which the target wire strand in that particular location was melted. In three of the perpendicular tests, no damage was seen to the wire strands. In the remaining ten tests, the results show that damage occurs directly above the arcing in some cases but in other the cases the plume is directed at an angle away from the power source. In all cases where damage was done to at least one strand in the TGS, the target in the first layer directly above the arc was damaged (in Figure 39 this would correspond with damage to wire location [1, 2]). No tests resulted in damage to target strands that were closer to the power source as compared to the arc location damaged.

4.5.3 ANALYSIS OF DAMAGE TO PASSIVE WIRES

Figure 41 is a plot of damage to the passive wire versus arcing energy. This data is from guillotine tests using 20 AWG, polyimide insulated active wires. The passive wires had various insulations. The damage scale is the same as the one used for the target wire at a distance. As expected, the graph shows that damage tends to increase with more arc energy. However the scatter in the data is large and a linear correlation coefficient with damage level and arc energy is 0.57. One reason for the scatter is that because the arc is directed away from the bundle the active wire tends to block the transfer of energy to the passive wires. The plot does shows that it required 20 J or more to do damage to the passive wire's primary insulation and more than 100 J to do significant damage (> 50% penetration of the insulation thickness).

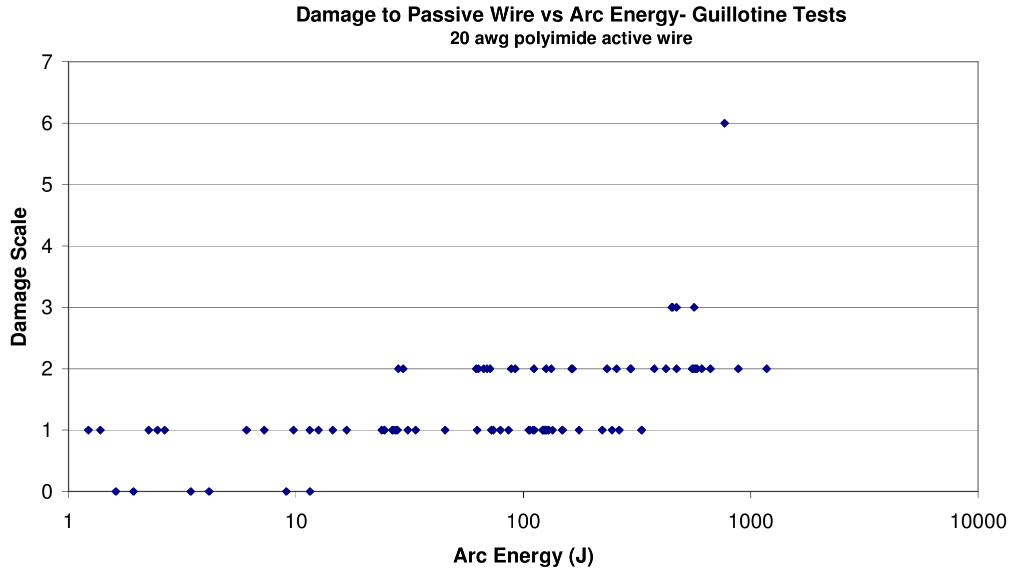

Figure 41. Damage to passive wire vs. arc energy for guillotine test.

5 CONCLUSION

The test plan proposed for laboratory testing phase of the project has been completed. A brief qualitative describing the results of each test group can be found in appendix B.

The data that was generated will be the foundation of the work to be performed in analytical phase (Task #2) of the project as well as the development of the arc damage modeling tool (Task #3). Task #2 will utilize the data to form analytical models addressing arc energy portioning, damage to targets and wires in the same bundle, and other items related to arc damage modeling. These methods will be developed such that they can be integrated into the arc damage modeling tool to be developed in Task #3. The initial analysis of the test data suggest the test parameters, arc characteristics and quantification of the damage has been captured in enough integrity and detail that it will be useful in creating models of arcing damage. The following were observed in the initial analysis of the data.

- For AC arcs the fault current is an important parameter in determining the energy dissipated in an arcing half cycle. The following chart shows the average energy in the arcing ½ cycles for different fault currents.

Fault Current (A)	50	100	250	300	500	1100
Average Energy in the Arcing 1/2 Cycle (J)	0.4	1.8	4.5	5.2	9.8	16.2

- As expected, there is a fairly strong correlation between arc energy and damage done to the target, active wire and passive wires.
- A large number of tests resulted in the penetration of hydraulic lines. These tests not only included those with high energy arcs and large diameter wires, but also some small gauge wires with lower energy arcs.

- The type of wire insulation had an effect on the damage done by the arc with wire that did not contain any polyimide showing the least damage. However, all wire types created damage in at least some cases.
- Arc fault circuit breakers significantly reduced the damage compared to thermal circuit breaker. However in some cases significant damage still can occur.
- Using a 28 VDC source voltage, arcing can penetrate an aluminum tube. This occurred more frequently with larger wire gauges (>20 AWG) and fault currents (> 400 amps).
- Testing that involved hydraulic lines occasionally resulted molten metal filling in penetrating damage areas, obfuscating the results of the damage depth probe.
- As the testing progressed, those performing the testing became prolific at igniting arcs. As such, there is a variation in the number of arcing half cycles seen in earlier tests.
- Thermal gradient stratification and the use of target wires at a distance proved to be a useful means of evaluating the effective damage radius of the arc plume. Initial results indicate that the damage distance is between ½" and ¾".
- There is significant scatter in the damage done to the passive wires in the bundle as compared to the energy in the arc. However, there does appear to be a minimum arc energy of around 200J to do significant damage to the passive wires.
- The vibration test proved to be a useful test, particularly in extending the duration of arcing events (by creating repeated strikes on the target, not one sustained arcing event. One of the disadvantages of this test however, was the long setup time compared to the other arc initiation methods.
- In many of the tests, the arc fault circuit breakers used were able to limit the damage done to the target. However, in a few of the test performed, the arcing was sufficient to penetrate the walls of hydraulic lines in spite of being protected with an AFCB.

APPENDIX A. TEST DESCRIPTIONS

A.1 SWING TEST

The swing test represents a ticking fault situation where a metal to metal contact is made momentarily and then separation occurs: for example, when a swaying bundle abrades the wire insulation and then the connector touches structure. The damage to arcing target was easily measured regardless if the target was structure, hydraulic lines, or flight control cables. Additionally, other wires in the bundle were easily measured. Because the insulation on the wire is pre-damaged, the duration of the test is short regardless of the target material.

The main purpose of this test was to record the damage (mass removed) done to the active wire conductor and to the target. In addition, the damage done to the other wires in the test harness was measured. The swing test, together with the vibration test was used to generate the vast majority of the dry arcing data. A diagram of the circuit can be seen in Figure A-1.

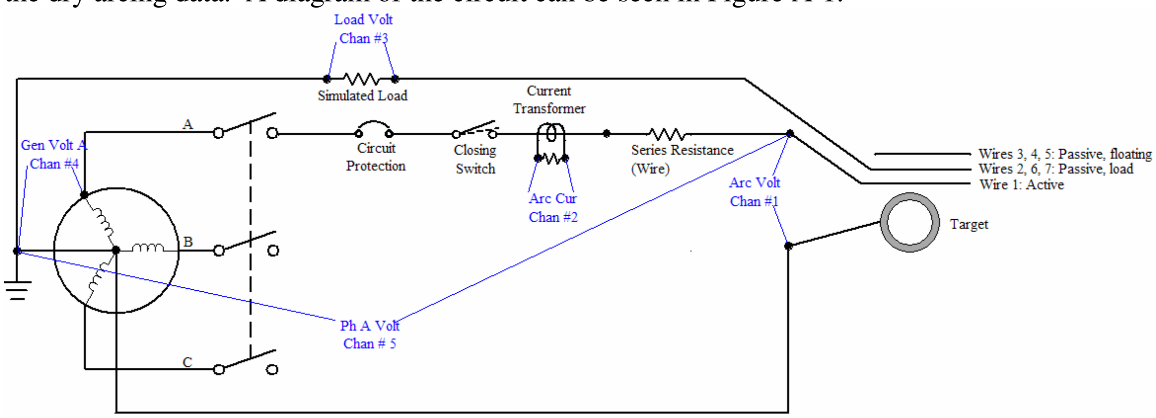

Figure A-1. Circuit diagram for the swing\vibration arc initiation method with an 115VAC power source.

A.2 VIBRATION TEST

The vibration test method represents the situation on the aircraft where a wire harness has come to lie on a metal piece of the aircraft and a wire chafes through and arcs to the metal object due to vibration. In the vibration test, an arc is created between a pre-damage wire on the outside of the test harness vibrating on a metallic target such as a hydraulic line, flight control cable or structural spar.

The main purpose of this test was to record the damage (mass removed) to the test wire conductor and to the target. In addition, the damage done to the other wires in the test harness was measured. The vibration test, together with the swing test, was used to generate the vast majority of the dry arcing data. A diagram of the circuit can be seen in Figure A-1.

In shakedown tests, the consistency of the results was improved if some of the test parameters were controlled. These parameters include the frequency and displacement of the vibration, and the force between the bundle and target. For a majority of the tests, the maximum resting weight of the wires on the target (the pre-vibration weight of wires at the bottom of the sinusoidal motion) was set to be within 10% of 100g. A small number of tests were carried out to investigate the damage with a variation in the maximum resting weight.

A.3 GUILLOTINE TEST

The guillotine test follow standard test methods with modifications as needed to meet the goals of the project. One change was to use thicker “blades” in addition to razor blades. In these tests, Al rectangles that are 1/16” or 1/8” in thickness were used. The edge of rectangles were not be sharpened so windows were cut into the active wire insulation to allow arc initiation. The main purpose of these tests were to measure damage to the target (blade) and the harness (passive wires). This test was also be used in the dirt and debris initiation tests and segregation tests.

This test procedure covers both the guillotine test procedures for grounded and non-grounded blades. Figure A-2 and Figure A-3 show the test circuits for each of the tests.

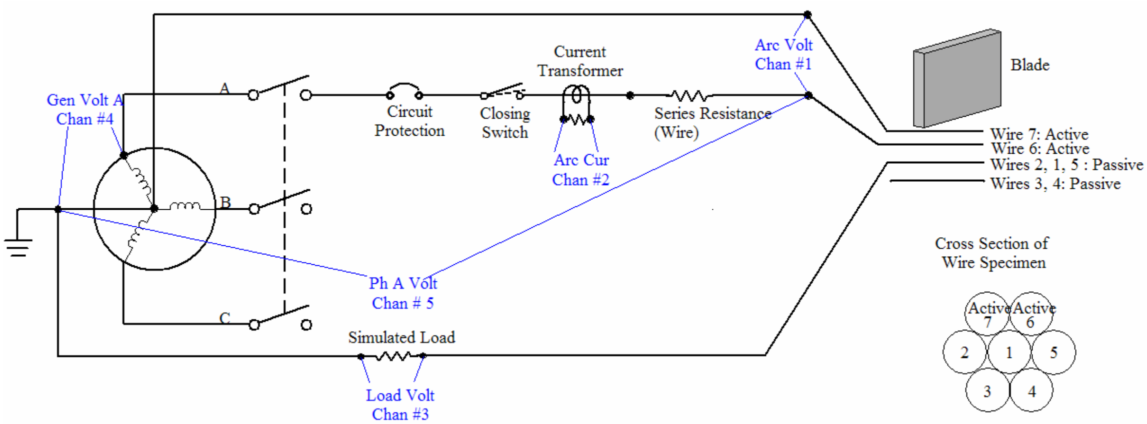

Figure A-2. Circuit diagram of ungrounded blade guillotine test.

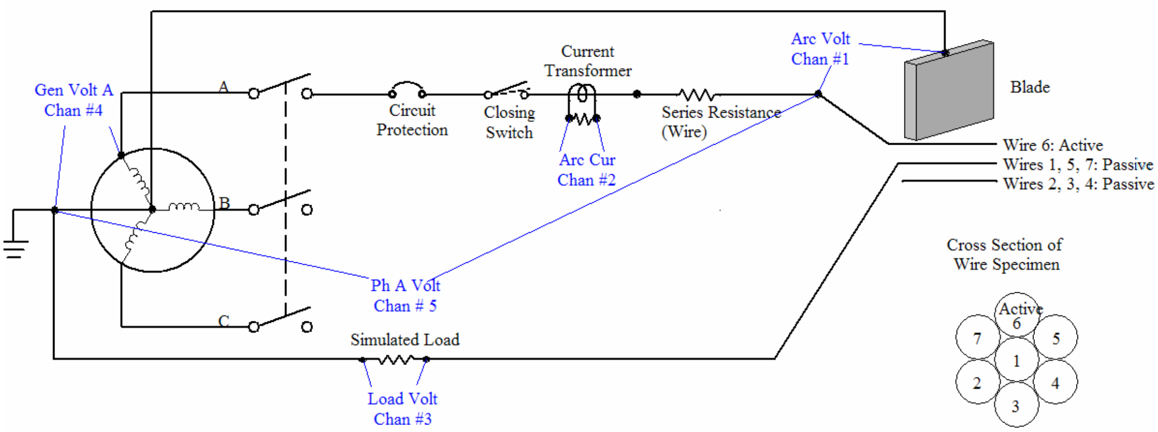

Figure A-3. Circuit diagram of grounded blade guillotine test.

The guillotine test was based on the wire test specification AS5692, but was modified to meet the objectives of this project. A seven wire bundle is constructed with a minimum of four tie-wraps to maintain the bundle shape and is affixed firmly to a Teflon block. A breach is made in the top two wires. These wires are arranged such that the breached wires were on top of the bundle; one wire connected to the voltage specified in the particular test configuration, the other wire connected to ground. A metallic blade (in the testing performed the blades used were steel razor blades, 1/16” and 1/8” aluminum blades) is then mounted on a fixture able to move in the up and down direction. The blade is then brought down to make contact with the exposed conductors of the top two wires in the bundle. The test is complete when the circuit breaker opens or when there is sufficient damage to the blade or wires that an electrical circuit can no longer be established.

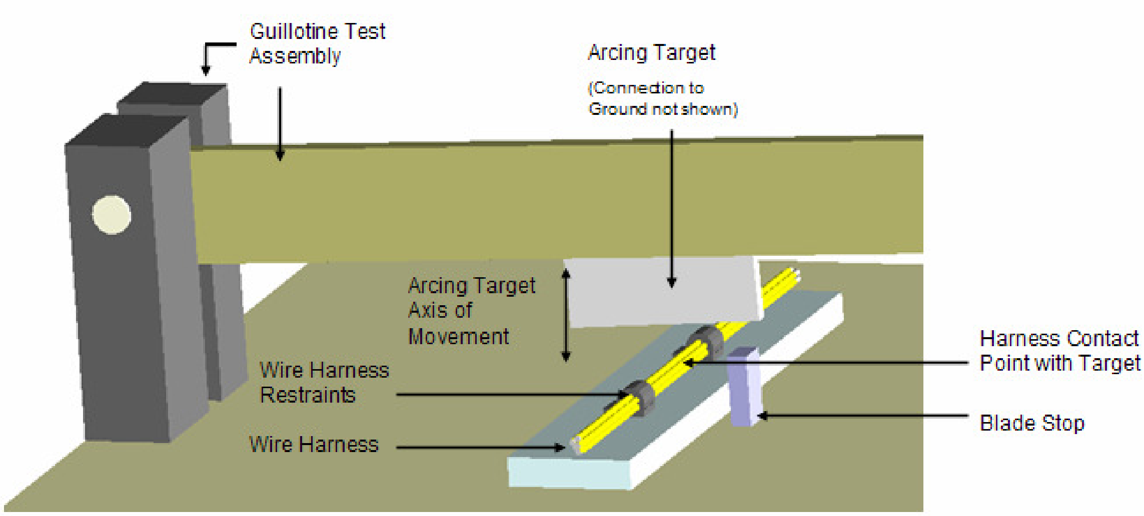

Figure A-4. Guillotine test apparatus.

The grounded guillotine test was designed to be similar to the guillotine test noted above with a couple of exceptions. In these tests, the bundles were constructed with only one wire with a breach in the insulation down to the conductor. Additionally, the blade is grounded and is the only grounded location in the test circuit.

A.4 WET TEST

The wet test represents a scenario in which fluid contamination creates an arc between two damaged wires (Figure A-5). In general, the tests follow the AS4373 Method 509 procedures with appropriate modification where were needed to meet the goals of this project. The main goal of these tests was to gather data on damage to the passive wires in the harness and damage to objects at a distance from the harness. Additionally, a measurement of the plume temperature at a distance from the harness was investigated using this method. A novel technique used to measure the plume temperature was the Thermal Gradient Stratification technique.

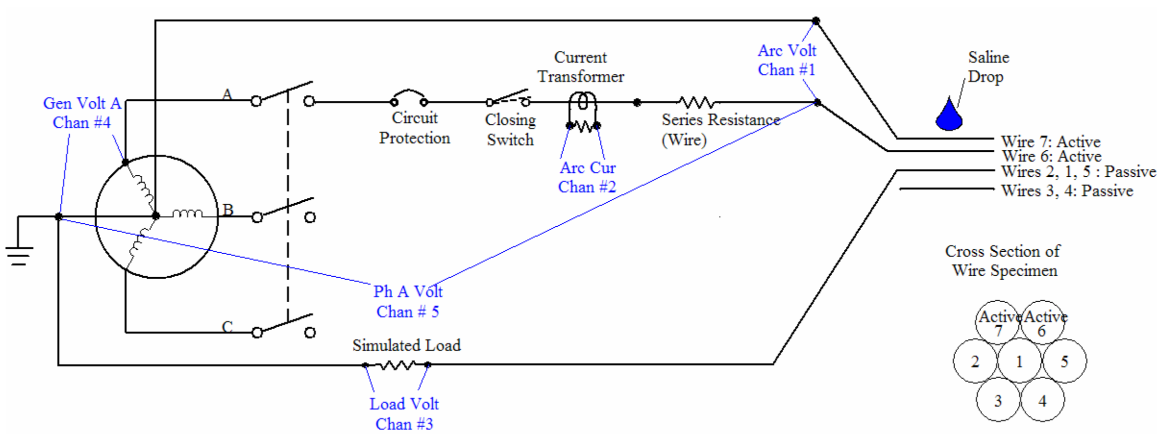

Figure A-5. Wet test circuit diagram for tests involving single phase configuration.

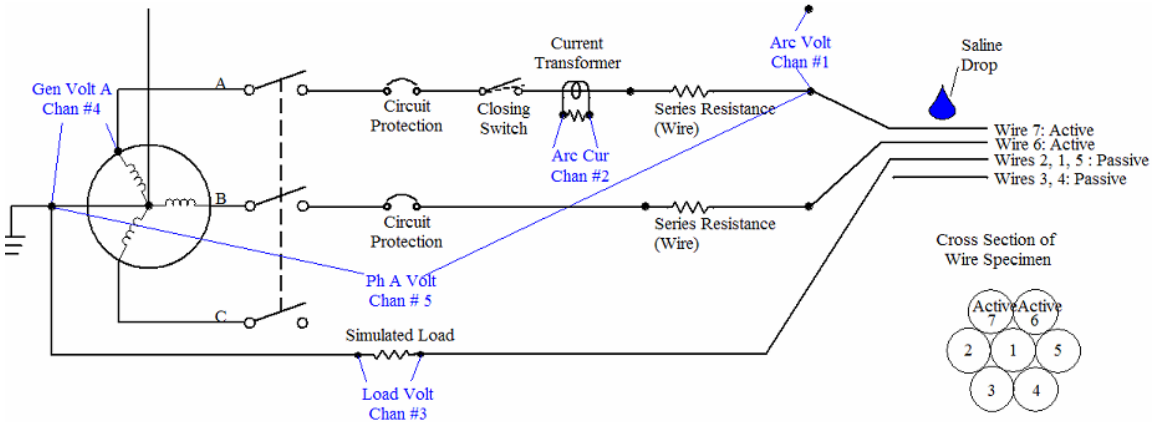

Figure A-6. Wet test circuit diagram for tests involving three phase test configuration.

A.5 FAULT CURRENT TEST

Separate from the tests, is the fault current test. This test was used in the testing as a means of assessing the maximum amount of current in the system if there were to be a short between the wire and the target. An example of this can be seen in Figure A-7.

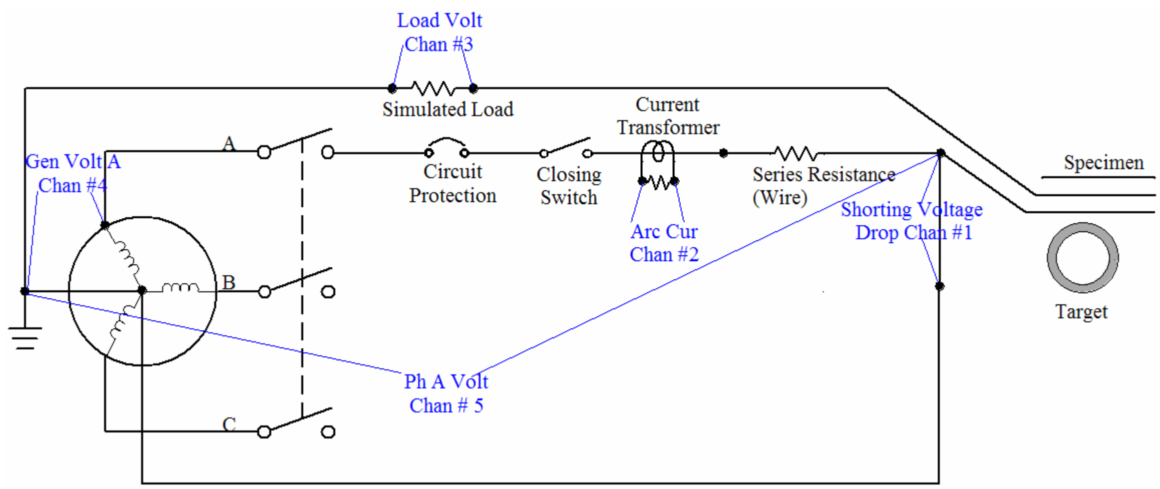

Figure A-7. An example diagram of the fault current test when applied to the swing\vibration test initiation method.

To perform the fault current test, the circuit was setup the same per the circuit diagram for the particular initiation method to be used, with the exception of the wire bundle removed from the circuit. A jumper wire was then placed between the active wire and the ground location (or in the case of the 3-phase tests, each phase was connected independently to ground). The power was then tuned on, and the current recorded. The setup was accepted if the fault current was within 5% of the desired fault current value for a test; resistance was added or removed as necessary to meet this goal.

APPENDIX B. DESCRIPTION OF TEST GROUPS

The following contains a brief qualitative describing the results of selected tests. Along with each selected test description are the parameters for the test group. The tests are organized by test group number.

Test Group	Test Category	Comment	Source Voltage	Active Wires	Passive Wires	Pre-damage to active Wire	Target	Initiation Method	Circuit Protection	Fault Current (A)
TG-003	Damage to Al Tube	Relatively consistent number of AHCs (all less than 10). Penetration in 1 of 6 tests. Some damage to passive wires seen in tests with more arc energy.	115 AC	81381/12-20	81381/12-20	1/2" Window	3/8" Al Tube	Swing	7.5 A Thermal	500
TG-007	Damage to Al Tube	There was a limited number of arcing half cycles in each test (<6), with a variation in damage from slight to penetration	115 AC	81381/12-20	81381/12-20	1/4" Sliver	3/8" Al Tube	Swing	7.5A AFCB	500
TG-008	Damage to FCC	Most tests (3 of the 4) resulted in minor damage to the FCC, with one test causing significant damage to one rope	115 AC	81381/12-20	81381/12-20	1/4" Sliver	Flight Control Cable	Swing	7.5 A Thermal	100
TG-018	Damage to Spar	Damage was seen in all tests with some material loss from the structure (no penetration).	115 AC	81381/12-20	81381/12-20	1/4" Sliver	Spar	Swing	7.5 A Thermal	900
TG-026	Damage to Ti Tube	No significant damage to tube	115 AC	81381/12-20	81381/12-20	1/2" Sliver	1/2" Ti Tube	Vibration	7.5A AFCB	100
TG-057	115 AC 1/8" Blade	Large variation in number of AHCs. Significant damage seen in tests with high number of AHCs (max 29.17mm^3). Large amounts of active wire damaged.	115 AC	81381/12-20	81381/12-20	1/2" Whole Cut	1/8" Al rectangle	Guil	7.5 A Thermal	250
TG-078	Damage to FCC	Some penetrating damage to the FCC was seen in all test. Some damage to active wires.	115 AC	81381/22-14	81381/22-14	1/4" Sliver	Flight Control Cable	Swing	15A AFCB	1100
TG-084	Damage to Ti Tube	Penetration in 2 of 3 tests. All tests had less than 8 AHCs.	115 AC	81381/22-14	81381/22-14	1/4" Sliver	1/2" Ti Tube	Swing	15A AFCB	1100

TG-093	Damage to Al Tube	Minor damage to tube; no significant penetration of the tube in any of the tests. In only one test was there significant damage to the active wire.	28VDC	81381/22-14	81381/22-14	1/4" Sliver	3/8" Al Tube	Swing	20 A Thermal	50
TG-109	Damage to Wire	Some damage to target wires; no more than one layer breached.	3Ph AC	81381/12-10	22759/34-10	Ring Cut	81381/22-20	Wet	20 A Thermal	1100
TG-115	Damage to Wire	All tests had below 11 AHCs. Damage to TGS seen at 0.25" in 1 of 3 test; remaining showed no damage.	115 AC	81381/12-20	81381/12-20	Ring Cut	Thermal Stratification	Wet	7.5A AFCB	250
TG-120	Damage to Wire	Relatively consistent number of AHCs. Minimal damage to target and active wires.	115 AC	81381/12-20	81381-12-20	Ring Cut	BMS1360-20	Wet	7.5 A Thermal	500
TG-123	115 AC 1/8" Blade	Significant damage to blades (minimum of 75 AHCs). Minimal damage to Teflon protection.	115 AC	81381/22-14	22759/34-14	1/4" Sliver	1/8" Al rectangle	Guil	20 A Thermal	500
TG-157	115 AC 1/8" Blade	High number of AHCs. Breach to conductor of passive wires in 2 of 3 tests; third test had noticeable damage to passive wire insulation.	115 AC	81381/12-20	AirBusCF-20	1/4" Sliver	1/8" Al rectangle	Guil	7.5 A Thermal	100
TG-166	Damage to Al Tube	Variation in number of AHCs. Some penetrating damage to tube, Minimal damage to passive wires.	115 AC	22759/34-20	22759/34-20	1/4" Sliver	3/8" Al Tube	Swing	7.5 A Thermal	250
TG-172	Damage to Al Tube	Low number of AHCs (all less than 3). Some penetrating damage to tube in 2 of 4 tests. Low damage to passive wires.	115 AC	22759/34-14	22759/34-14	1/4" Sliver	3/8" Al Tube	Swing	20A AFCB	500
TG-200	Damage to Al Tube	Weight on Tube :150g - Penetration in 2 of 3 tests. Some damage to passive wires.	115 AC	81381/12-20	81381/12-20	1/4" Sliver	3/8" Al Tube	Vibration	7.5 A Thermal	250
TG-304	TGS	Damage to 2nd layer in one test, and to 1st layer in 2 of 3 test. No damage to TGS in last test.	115 AC	81381/12-20	81381-12-20	Ring Cut	Thermal Stratification	Wet	7.5A AFCB	500